BNL--51798

DE85 018052

BNL 51798
UC-94d
(Energy Storage-Chemical — TIC-4500)
MIT/BNL 83-3

HIGH-TEMPERATURE STEAM ELECTROLYSIS: TECHNICAL AND ECONOMIC EVALUATION OF ALTERNATIVE PROCESS DESIGNS

M.A. Liepa and A. Borhan

Consultants: G.T. Skaperdas, A. Mezzina, and F.J. Salzano

September 1983

BROOKHAVEN STATION
SCHOOL OF CHEMICAL ENGINEERING PRACTICE
MASSACHUSETTS INSTITUTE OF TECHNOLOGY
T.A. HATTON, DIRECTOR
A.D. RICHARDS, ASSISTANT DIRECTOR

TECHNOLOGY BASE PROGRAMS
DEPARTMENT OF APPLIED SCIENCE
BROOKHAVEN NATIONAL LABORATORY
ASSOCIATED UNIVERSITIES, INC.
UPTON, LONG ISLAND, NEW YORK 11973

UNDER CONTRACT NO. DE-AC02-76CH00016 WITH THE
UNITED STATES DEPARTMENT OF ENERGY

Printed in the United States of America
Available from
National Technical Information Service
U.S. Department of Commerce
5285 Port Royal Road
Springfield, VA 22161

NTIS price codes:
Printed Copy: A05; Microfiche Copy: A01

DEDICATION

The Brookhaven Station of the MIT School of Chemical Engineering Practice was established in the summer of 1983. It represents a new direction for the Laboratory which could not have been implemented without the strong support and encouragement of our former Deputy Director, the late Dr. Warren E. Winsche. Establishment of the station at BNL embodies three of Dr. Winsche's interests during his long and notable career in chemical engineering and research management. These are the continued pursuit of the high standards of professional chemical engineering practice; the role of the National Laboratories in providing both facilities and staff to assist in the training of engineers and scientists; and thirdly, and perhaps most important, an appreciation for the stimulus and fresh ideas often provided by students and those still in a "learning" mode, as an essential to the well being of any research organization.

These reports amply demonstrate the above characteristics and represent only a portion of the success of the first year of operation of the station.

We expect this cooperative effort between BNL and MIT to continue well into the future and for this we gratefully dedicate these reports to the memory of Dr. Winsche.

ABSTRACT

A high-temperature water-vapor electrolysis (HTE) unit operating at an average temperature of 1000°C (1832°F) was integrated into a preliminary process design using electrical and thermal energy derived from coal. Process variations with either steam or water feed and either isothermal or nonisothermal HTE operation were considered. Operating and capital costs were estimated for each process flowsheet, with the lowest costs being obtained for operation with high steam conversions in the electrolyzer. Estimated hydrogen production costs were compared with estimates obtained from the literature for other hydrogen production processes. The estimated HTE hydrogen production costs were in the range \$0.17 to \$0.22/m^3 H_2 (\$14 to \$18/10^6 Btu), assuming \$2/10^6 Btu for thermal energy and \$0.05/kWh for electrical energy.

CONTENTS

TABLES

FIGURES

1 SUMMARY

Manufacturing hydrogen by electrolyzing water vapor at high temperatures has potential cost advantages over lower temperature processes because a portion of the endothermic heat of reaction can be supplied thermally rather than electrically. As an illustration, using the thermal energy of coal directly at a cost of $2/10^6$ Btu would be more than seven times less expensive than generating electricity from that same coal and then using the energy at a cost of $0.05/kWh. This cost reduction is being made possible through the development of high-temperature steam electrolysis cells by a number of research groups [Doenitz et al. (1980) and Westinghouse Electric Corp. (1983)]. These cells have a solid-oxide electrolyte and operate at temperatures above about 900°C (1652°F).

In our study, a high-temperature steam electrolyzer (HTE) operating at an average temperature of 1000°C (1832°F) was integrated with a coal-fired thermal energy source at about 2000°C (3632°F). Heat recovery equipment for preheating the electrolyzer feed stream with the thermal energy of the electrolyzer product streams was also included in our preliminary designs. The hydrogen production rate at 25°C (77°F) and 3 atm was specified to give a higher heating value of 10 MW_t. This production rate was chosen to limit the electrolysis plant electricity requirements to only about one percent of the peak electrical output of a coal-fired 1000-MW_e power plant. This limitation would be appropriate for an HTE demonstration plant built adjacent to that power plant.

Three basic process designs were considered. These designs will be referred to in the following discussion as Processes A, B, and C. Table (1-1) shows typical HTE hydrogen production costs obtained through our technical and economic evaluation of each of the processes. The thermodynamic efficiency with which the thermal energy of coal can be converted into hydrogen is also shown. The assumptions on which these results are based are given at the bottom of the table.

The ASPEN-PLUS process simulator program [Aspen Technology, Inc. (1983)] was used to calculate material and energy balances for each of the processes. Thermal and electrical power requirements were calculated with an error of less than 0.01% by this program. Capital cost estimates were then obtained using the techniques recommended by Peters and Timmerhaus (1980). These estimates were only accurate to within about 30%, but this represents a potential hydrogen production cost error of just $\$0.01/m^3$ H_2 produced ($\$0.8/10^6$ Btu) because capital cost accounts for only about 20% of the HTE hydrogen production cost.

In the first process design considered, Process A, 153°C (307°F) saturated steam was preheated by heat recovery and then reacted isothermally. In this case, all of the endothermic heat of reaction was provided electrically. This base case resulted in an upper bound on hydrogen production cost and a lower bound on thermodynamic efficiency. We estimated hydrogen production costs from purchased steam of $\$0.24/m^3$ H_2 produced ($\$20/10^6$ Btu) for a steam conversion of 30% in the electrolyzer and $\$0.19/m^3$

Table (1-1)
Comparison of HTE Processes

Process	Feed	Electrolyzer Operation	Steam Conversion Fraction	Production Cost ($/m^3 H_2)	Production Cost ($/$10^6$ Btu)	Thermodynamic Efficiency (%)
A	Steam	Isothermal	0.30	0.22 (0.24*)	18 (20*)	31.9
			0.90	0.19 (0.19*)	16 (16*)	36.9
B	Steam	Nonisothermal	0.30	0.18 (0.20*)	15 (17*)	34.7
			0.90	0.17 (0.18*)	14 (15*)	38.2
C	Water	Nonisothermal	0.30	0.21	18	38.5

*Including Steam Cost of 0.69¢/kg ($3.10/1000 lbm).

Basis: Electrical Energy Cost = $0.05/kWh
Thermal Energy Cost = $2/$10^6$ Btu
20% Annual Capital Recovery Charge
Hydrogen Product 10 MW_t, 25°C (77°F), 3 atm
Thermodynamic Efficiency of Electrical Power Generation = 35%
Thermodynamic Efficiency of Steam Generation = 100%
Hydrogen Volume Measured at 0°C (32°F), 1 atm

H_2 ($16/$10^6$ Btu) for a 90% conversion. Assuming a 35% efficiency for electrical power generation from coal, hydrogen production efficiencies from coal of 31.9% for a 30% steam conversion and 36.9% for a 90% conversion were calculated.

In Process B, part of the heat of reaction was provided thermally by preheating the feed steam to 1100°C (2012°F) in ceramic tubes installed in the radiant zone of a coal-fired furnace and then allowing a 200°C (360°F) temperature drop in the electrolyzer. Hydrogen production costs from purchased steam were reduced to $0.20/$m^3$ H_2 produced ($17/$10^6$ Btu) for a steam conversion of 30% and $0.18/$m^3$ H_2 ($15/$10^6$ Btu) for a 90% conversion. Thermodynamic efficiencies were improved to 34.7% for a 30% steam conversion and 38.2% for a 90% conversion.

In Process C, feed water was boiled at 1 atm by recovering the heat of condensation of water remaining in the product stream. The 100°C (212°F) saturated steam was then compressed to a pressure of about 5 atm so that condensation in a later step would occur above 110°C (230°F). For the same electrolyzer temperature and pressure as in Process B, the hydrogen production cost increased to $0.21/$m^3$ H_2 produced ($18/$10^6$ Btu) for a 30% steam conversion because of steam compression cost. The thermodynamic efficiency for a 30% conversion increased to 38.5%, however, because of greater heat recovery from the product gases. A maximum conversion of 35% was obtained for a hydrogen product pressure of 3 atm because too much condensation occurred below 110°C. Increasing this pressure increased the maximum conversion but also increased the electrical power required for steam compression. For example, a hydrogen product pressure of 10 atm was enough to reduce thermodynamic efficiency from 38.5% to 35.6% for a steam conversion of 30%.

The results for Processes B and C could be further improved by introducing interstage reheating between electrolyzers having 200°C temperature drops. In this way thermal energy input is maximized by reducing the electrical energy input to only that required for electrolysis. Reheating between staged electrolyzers could decrease the hydrogen production costs given in Table (1-1) for Processes B and C from $0.01 to $0.02/$m^3$ H_2 produced ($0.8 to $2/$10^6$ Btu). This represents a 5% to 10% savings.

Steam reforming of natural gas is currently the least expensive way to manufacture hydrogen. Production costs range from about $0.08 to $0.11/$m^3$ H_2 produced ($7 to $9/$10^6$ Btu), based on a natural gas cost of $3.50/$10^6$ Btu. If the price of natural gas were to increase to $8/$10^6$ Btu, however, hydrogen production costs for steam reforming would increase to about $0.16 to $0.20/$m^3$ H_2 ($13 to $17/$10^6$ Btu). This cost range is comparable to the one we estimated for HTE hydrogen production, which was $0.17 to $0.22/$m^3$ H_2 produced ($14 to $18/$10^6$ Btu).

2 INTRODUCTION

2.1 Background and Motivation

Plentiful, low cost supplies of transportable fuels, required in industry, are currently derived from oil and gas deposits. Naturally occurring liquid and gaseous hydrocarbon reserves are finite, however, and will eventually be depleted. Liquid and gaseous fuels will have to be supplied synthetically from nonconventional fossil sources such as oil shale and coal or from nonfossil resources.

A fuel with great potential availability is hydrogen originating from a water source. The possibility of using hydrogen as an energy carrier instead of fuels such as gasoline and natural gas has received widespread attention in recent years [Mandelik and Newsome (1980)]. Hydrogen can be used directly as a gaseous or liquid fuel or it can be chemically transformed into other transportable fuels like methanol, methane, gasoline, or oil by combining it with a renewable carbon source such as biomass or atmospheric carbon dioxide.

A hydrogen-based economy requires a highly efficient and low cost process for hydrogen production. Currently, the principal commercial processes for hydrogen manufacture are catalytic steam reforming of methane, partial oxidation of liquid hydrocarbons such as naphtha, coal gasification, and water electrolysis. A brief review of these processes is given in the sections which follow to provide a basis and rationale for considering an alternative process: high-temperature steam electrolysis (HTE).

2.2 Hydrogen Production from Fossil Fuels

Hydrogen is produced commercially from fossil fuels by the following reactions [Mandelik and Newsome (1980)]:

Steam Reforming of Methane $CH_4 + 2\ H_2O \longrightarrow CO_2 + 4\ H_2$

Resid Partial Oxidation $CH_{1.8} + 0.98\ H_2O + 0.51\ O_2 \longrightarrow CO_2 + 1.88\ H_2$

Coal Gasification $CH_{0.8} + 0.6\ H_2O + 0.7\ O_2 \longrightarrow CO_2 + H_2$

In the United States, the bulk of the industrial hydrogen is manufactured by steam reforming of natural gas. Relatively small quantities of hydrogen are being produced by steam reforming of naphtha and by partial oxidation of oil.

The principal disadvantage of the partial oxidation process is that 95% to 99% pure oxygen is required. Ordinarily, this is supplied by an air separation plant which adds appreciably to the operating cost and possibly

the capital cost (that is, if a new air separation plant is built). However, the partial oxidation process can utilize any gaseous or liquid hydrocarbon feedstock. This would include hydrocarbon cuts from natural gas to crude oil, residual oil, or even asphalts or waxes. No desulfurization is required prior to the partial oxidation step whereas in the reforming process the catalyst requires a desulfurized hydrocarbon feed [Mandelik and Newsome (1980)]. Consequently, partial oxidation plants are installed primarily in locations where natural gas or lighter hydrocarbons, including naphtha, are uneconomical as compared with heavier residual fuel oil or crude oil. At the present time there are only two plants in the United States using partial oxidation of hydrocarbons to produce hydrogen [Mandelik and Newsome (1980)].

In general, as the molecular weight of the feedstock increases from natural gas to liquid hydrocarbons and then to solid residuals, processing difficulties and manufacturing costs increase. Partial oxidation and coal gasification processes require more capital investment than the steam reforming plants because an air separation plant, larger CO_2-removal facilities, and gas cleanup are needed.

Although steam reforming and partial oxidation processes are currently the most economical means of hydrogen production, with a hydrogen production cost of about \$0.08 to \$0.13/m^3 H_2 produced (\$7 to \$11/10^6 Btu) [Gregory et al. (1980)], they are not suitable processes for a hydrogen-based economy since they require gaseous and liquid hydrocarbon feedstocks. Because hydrogen production cost is strongly controlled by oil and natural gas costs in these processes, they will become less economical as the supplies of gaseous and liquid hydrocarbons become more expensive. A suitable alternative is hydrogen production by water electrolysis.

2.3 Hydrogen Production by Water Electrolysis

Electrolysis of aqueous solutions of potassium hydroxide at near-ambient temperatures is used to produce hydrogen if an inexpensive electrical power source, such as a hydroelectric dam, is available or if only small quantities of pure hydrogen are required. However, there are thermodynamic restrictions to the overall process efficiency. Total efficiencies of conventional water electrolysis plants are limited to 25% to 28% with respect to the primary heat source used for electrical power generation (based on a 74% electrolysis efficiency combined with a 33% to 38% thermal efficiency for electrical power generation) [Doenitz et al. (1980)]. The actual electrical power consumption of conventional electrolysis cells is approximately twice the theoretical minimum electrical power requirement, which corresponds to the free energy of reaction (ΔG) at the operating temperature. This high consumption is due to overpotentials at the electrodes. Even with an electrolysis cell efficiency of 100%, the overall efficiency of this process would be limited to 33% to 38%. As a result of the inefficiency, electrolytic hydrogen is currently too expensive for general use.

There are thermodynamic advantages to performing water electrolysis at very high temperatures, typically 900° to 1100°C (1652° to 2012°F), as shown in Fig. (2-1) [Doenitz et al. (1980)]. The total energy demand (ΔH) for water decomposition is lower in the vapor phase than in the liquid phase. The difference is mostly the enthalpy of vaporization of water and can be provided thermally instead of electrically. In addition, the minimum demand for electrical energy, ΔG, needed for electrolysis decreases with increasing temperature. It is also possible to provide part of the water decomposition energy thermally instead of electrically, thus achieving higher total efficiencies. Because ΔG decreases with increasing temperature, the reversible potential of the electrolysis cell also decreases. Furthermore, improved reaction kinetics at elevated temperatures reduce electrode overpotentials. Hence, since the amount and cost of electricity needed to make hydrogen from water is proportional to the electromotive force of the cell, the cost of hydrogen production decreases with increasing temperature.

The feasibility of using high-temperature solid-oxide electrolytes for electrolysis of water vapor has been demonstrated by a number of research groups [Doenitz et al. (1980) and Westinghouse Electric Corp. (1983)]. Preliminary experiments performed by Westinghouse at 1000°C (1832°F) in ceramic electrolyte cells showed that high-temperature steam electrolysis (HTE) can be carried out at much lower cell potentials than those required by conventional electrolysis [Westinghouse Electric Corp. (1983)].

In the HTE process, steam is generated and then heated to above 1000°C. The water vapor is split into hydrogen and oxygen in the electrolysis cell according to the following reactions:

Cathodic Reaction $\quad 2\ H_2O_{(g)} + 4\ e^- \longrightarrow 2\ H_{2(g)} + 2\ O^{2-}$

Anodic Reaction $\quad 2\ O^{2-} \longrightarrow O_{2(g)} + 4\ e^-$

Figure (2-2) shows a cross-section of an electrolysis membrane. A gas-tight electrolyte of yttria-stabilized zirconia is sandwiched between the porous cathode and anode. The cathode consists of a cobalt or nickel cermet with 50 vol % zirconia as the ceramic. The anode is typically a modified lanthanum manganese oxide. Water vapor dissociates under the influence of an external electrical field at the cathode. Hydrogen molecules form at the cathode while oxygen ions, following the electrical field, migrate through the electrolyte and form oxygen molecules at the anode. The products, hydrogen and oxygen, are kept separated by the gas-tight electrolyte. The oxygen partial pressure on the hydrogen side of the electrolysis membrane is between 10^{-16} and 10^{-12} atm at 1000°C [Doenitz et al. (1980)].

Considerable thermal energy remains in the hot electrolyzer product streams. This energy must be recovered to maximize the thermodynamic efficiency of the process. For example, heat exchangers can be used to superheat the feed steam while cooling the product streams.

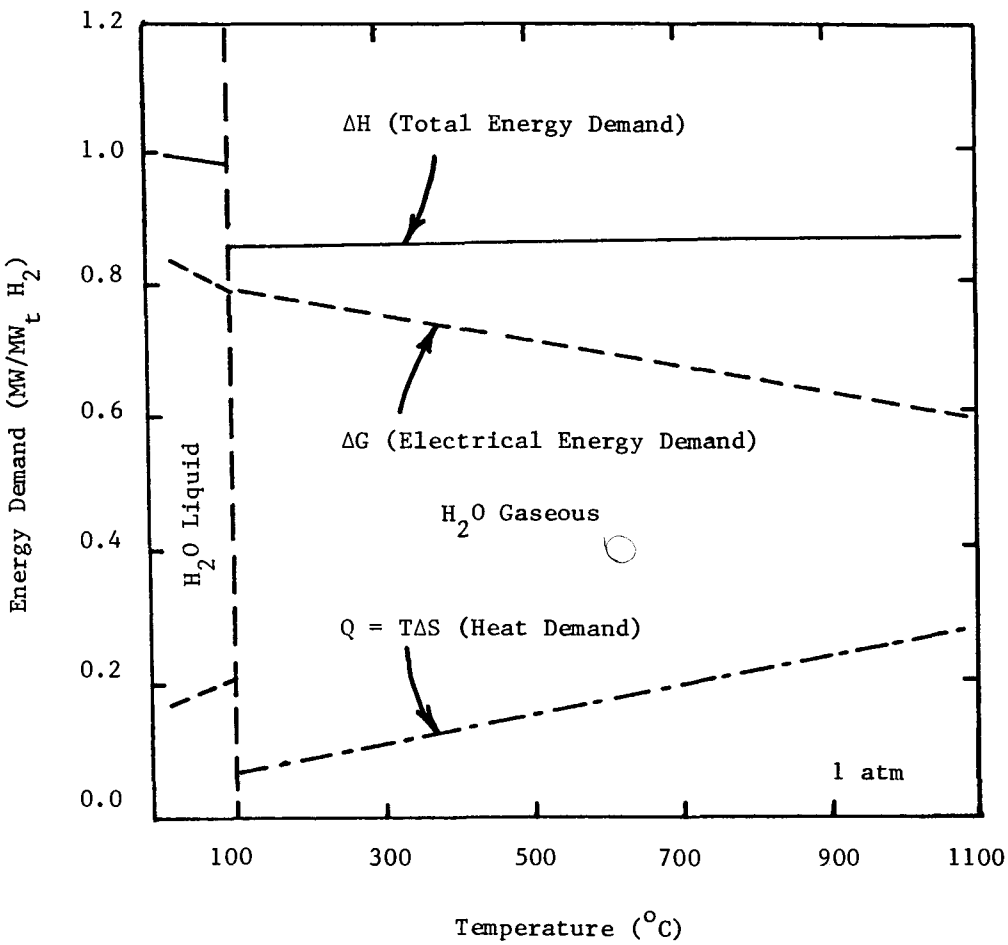

Thermodynamics of Water Splitting
[Doenitz et al. (1980)]

MASSACHUSETTS INSTITUTE OF TECHNOLOGY SCHOOL OF CHEMICAL ENGINEERING PRACTICE			
DATE 8-27-83	DRAWN BY AB	FILE NO MIT-BNL-83-3	FIG 2-1

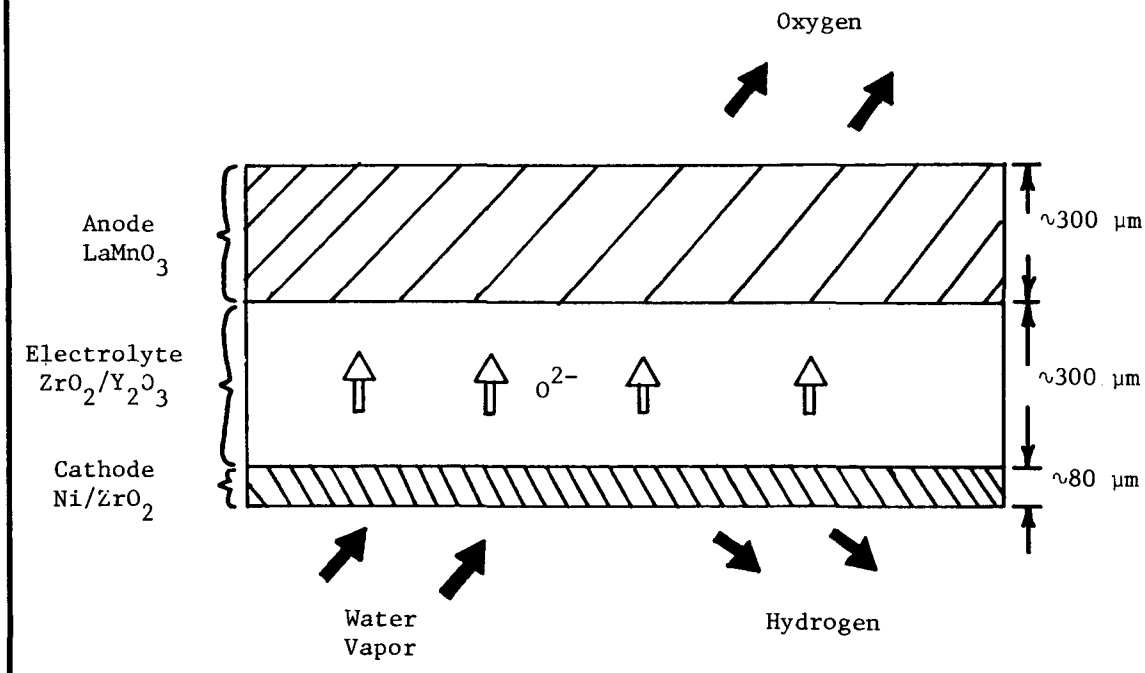

Cross-Section of a High-Temperature Steam Electrolysis Membrane

MASSACHUSETTS INSTITUTE OF TECHNOLOGY SCHOOL OF CHEMICAL ENGINEERING PRACTICE			
DATE 8-27-83	DRAWN BY AB	FILE NO. MIT-BNL-83-3	FIG 2-2

Many types of primary energy sources could possibly be coupled with a HTE process. These include fossil sources like coal or oil shale and inexhaustible energy sources like fission, fusion, or solar. Various processes for producing hydrogen from fusion energy have been examined and the most promising appears to be HTE [Booth (1979), Powell (1979), and Fillo (1983)].

Since fusion energy is not yet available, any current development of a HTE process must rely on an available primary energy source such as coal. In addition, before HTE can be commercially implemented, a significant amount of process design work must be done. The overall process design for HTE is more complicated than that for conventional electrolysis because of the high operating temperatures. The heat content of the product gases would have to be recovered by heat exchange with the feed steam to reduce the net energy input required. The feed steam would then be heated above 1000°C by a high-temperature heat source which, in principle, can be entirely independent of the electrical power source for the electrolysis cells. Integration of HTE with a heat recovery system and high-temperature heat source must also be done in a way which minimizes hydrogen production cost.

2.4 Objectives and Approach

Our first objective was to develop preliminary process designs which integrated a HTE unit with a thermal energy source and heat recovery equipment. The thermal energy source selected was a coal-fired furnace operating at about 2000°C (3632°F). The average electrolyzer operating temperature was assumed to be 1000°C (1832°F). Heat exchangers were used to preheat the electrolyzer feed stream while cooling the hot product streams. We developed several alternative HTE process flowsheets (see Section 4.1). Particular emphasis was given to replacing the use of electricity derived from coal with the less expensive direct use of coal-fired heat since this was expected to reduce hydrogen production cost significantly.

Our second objective was to analyze the economics of the alternative HTE processes we selected. To accomplish this, we first calculated material and energy balances for each process flowsheet. Electrolyzer steam conversions of 15% to 90% and hydrogen product pressures of 3 to 10 atm were considered. We then estimated operating and equipment costs based on the material and energy balance results (see Section 4.2). Finally, the HTE hydrogen production cost estimates we developed were compared with production costs obtained from the literature for other hydrogen manufacturing processes [Corneil and Heinzelmann (1980), Gregory et al. (1980), and Gupta and Russell (1981)].

3 PROCESS DESIGN BASIS AND ASSUMPTIONS

In this section we present the basis and assumptions used in developing and analyzing our preliminary high-temperature water-vapor electrolysis (HTE) process design flowsheets. The first part gives the design basis and the second gives the assumptions made while analyzing the processes.

3.1 Process Design Basis

Our process design basis was a hydrogen production rate of 0.0705 kg/sec (560 lbm/hr), or 0.784 m^3/sec (1660 ft^3/min) at 0°C (32°F) and 1 atm. This hydrogen production rate has a thermal heating value of 10 MW (34.1 x 10^6 Btu/hr) if both the heat of hydrogen combustion and the heat of condensation of the steam combustion product can be extracted to 25°C (77°F). This hydrogen production rate was chosen to limit the electrolysis plant electrical power requirements to only about one percent of the peak electrical output of a coal-fired 1000-MW_e power plant. This limitation would be appropriate for an HTE demonstration plant built adjacent to that power plant.

Because our HTE process design was on a demonstration plant scale, we assumed that the coal-fired power plant supplying electricity to our electrolysis plant would also have a boiler available to supply 153° to 189°C (307° to 372°F) saturated steam. In addition, this boiler would be able to supply thermal energy at about 2000°C (3632°F). We also assumed that treated process or cooling water could be obtained from the adjacent power plant.

In addition to the hydrogen product, the HTE process produces a pure oxygen byproduct. In our case, the oxygen production rate was 0.560 kg/sec (4440 lbm/hr), or 0.392 m^3/sec (830 ft^3/min) at 0°C and 1 atm. We only considered the oxygen byproduct stream to the extent necessary for heat recovery equipment design. Our hydrogen production cost estimates might be reduced further if the oxygen could be sold. Additional oxygen processing equipment would then be necessary, however. In any event, the hot oxygen byproduct stream could always be used to replace part of the preheated air normally used in the coal-fired furnaces of the adjacent power plant.

3.2 Process Design Assumptions

The major assumptions made in our preliminary HTE process design are summarized in Table (3-1). Additional minor assumptions are given in the description of our flowsheet analysis methods (see Section 4.2).

The minimum hydrogen concentration in the high-temperature electrolyzer was 5 mol % to prevent oxidation of cobalt-zirconia cermet electrolysis-cell cathodes [Mezzina (1983)]. This requirement led to the inclusion of a hydrogen recycle stream in all process flowsheets. Use of nickel-zirconia cermet cathodes could potentially reduce or eliminate that recycle stream [Mezzina and Bonner (1983)].

Table (3-1)
Major Process Design Assumptions

1. Feed stream to HTE at least 5 mol % hydrogen, with the balance steam.
2. Average HTE temperature of 1000°C (1832°F).
3. Maximum HTE temperature drop of 200°C (360°F).
4. High-temperature ceramic equipment only exposed to gases at less than 12 atm.
5. No heat addition to process below 900°C (1652°F).
6. Treated cooling and feed water available at 15°C (59°F).
7. Minimum temperature approach in heat exchangers of 10°C (18°F).
8. Pressure drop of 34.5 kPa (5 psi) in each piece of process equipment.
9. Hydrogen product stream leaves plant at 25°C (77°F) saturated with water vapor.
10. Hydrogen insoluble in water.

The average electrolyzer temperature was 1000°C (1832°F) to give good oxygen ion conductivity in the solid-oxide electrolyte. For nonisothermal electrolyzer operation, a maximum temperature of 1100°C (2012°F) was chosen to minimize materials problems, while a minimum temperature of 900°C (1652°F) was chosen to minimize conductivity loss in the electrolyte. As a result, the maximum temperature drop was 200°C (360°F).

Because of the high electrolyzer operating temperatures, the feed gases must be preheated to 1100°C in ceramic tubes. As a result, high operating pressures cannot be used. The hydrogen product pressures we considered were 3 to 10 atm. In addition, evaporating 100° to 152°C (212° to 306°F) water in 1000°C ceramic tubes might cause materials problems so ceramic process equipment was only exposed to gas streams.

We assumed that 153° to 189°C (307° to 372°F) saturated steam could be supplied by the adjacent power plant and that high-temperature thermal energy could be extracted by running ceramic tubes through the radiant section of a coal-fired furnace in that plant. The construction of a new furnace to provide both low- and high-temperature process heat was therefore not considered. We also assumed that treated water at 15°C (59°F) could be purchased from the power plant, so new cooling towers and water-softening equipment would not have to be built. The cooling water requirement for the electrolysis plant depended on steam conversion in the electrolyzer, but was usually less than 15 kg/sec (240 gal/min).

A minimum temperature approach of 10°C (18°F) was used in heat exchangers to avoid pinch points in condensers and boilers. Using a 10°C approach and conservative overall heat transfer coefficient estimates led to the design of very large gas-gas heat exchangers, however. A larger temperature approach in these exchangers would have reduced our capital cost estimates. We also assumed an average pressure drop of 34.5 kPa (5 psi) in all heat transfer equipment and in the high-temperature electrolyzer. This pressure drop is lower than that needed for good heat transfer in gas-gas exchangers but higher than that usually obtained in boilers and condensers [Peters and Timmerhaus (1980)].

Because of the temperature approach restriction and cooling water temperature chosen, the minimum hydrogen product temperature was 25°C (77°F). The maximum water content of this stream after condensation separation at 25°C was found to be 1.04 mol % at a total product pressure of 3 atm, so the cost of additional drying equipment was not considered. The solubility of hydrogen in water was also neglected since its maximum value at the maximum product pressure of 10 atm was about 0.014 mol % [Perry and Chilton (1973)].

4 PROCESS FLOWSHEET SELECTION AND ANALYSIS

This section describes the selection and analysis of our preliminary high-temperature steam electrolysis (HTE) process design flowsheets. The first part presents the flowsheets we analyzed. The second part gives an example analysis of process material and energy balances and of process economics.

4.1 Selection of Process Flowsheets

A flowsheet for the HTE process which we selected as a base case, Process A, is shown in Fig. (4-1). In Process A, 153° to 189°C (307° to 372°F) saturated steam is heated to about 1000°C (1832°F) and then electrolyzed isothermally with electricity derived from coal. No ceramic steam-preheating tubes are run through a coal-fired furnace, so all of the high-temperature energy input must be provided electrically. Process A was selected as our base case because the high electrical power consumption gave an upper bound on hydrogen production cost. It also gave a lower bound on the thermodynamic efficiency with which the thermal energy of coal can be converted into hydrogen. An example analysis of the flowsheet is given in Section 4.2, while a summary of all analyses of Process A is given in Section 5.1.

A flowsheet for the second HTE process we considered, Process B, is shown in Fig. (4-2). In Process B, low-pressure saturated steam is again fed to the HTE plant. The steam is first preheated and then heated to 1100°C (2012°F) in ceramic tubes installed in the radiant section of a coal-fired furnace. For our assumed 10-MW_t hydrogen production rate, the required furnace duty is about 1 to 2 MW_t (3 to 7 x 10^6 Btu/hr). Finally, the steam is electrolyzed with an accompanying temperature drop of 200°C (360°F). In this way some electrical power input is replaced by thermal energy. As a result of this substitution, Process B had a lower hydrogen production cost than Process A. The cost was lower because direct use of coal-fired heat is less expensive than using electricity derived from coal. In addition, the thermodynamic efficiency of Process B was greater than that of Process A because of the direct use of thermal energy. A summary of the results obtained for Process B is given in Section 5.2.

A flowsheet for the third HTE process we considered, Process C, is shown in Fig. (4-3). In Process C, steam is generated from water and preheated by heat exchange with the product gases before again being heated to 1100°C by a coal-fired furnace. The remainder of Process C is the same as Process B. We studied Process C to determine the effect of additional heat recovery equipment on hydrogen production cost. Maximizing heat recovery from the product streams gave Process C a better thermodynamic efficiency than Process B. A summary of all analyses of Process C is given in Section 5.3.

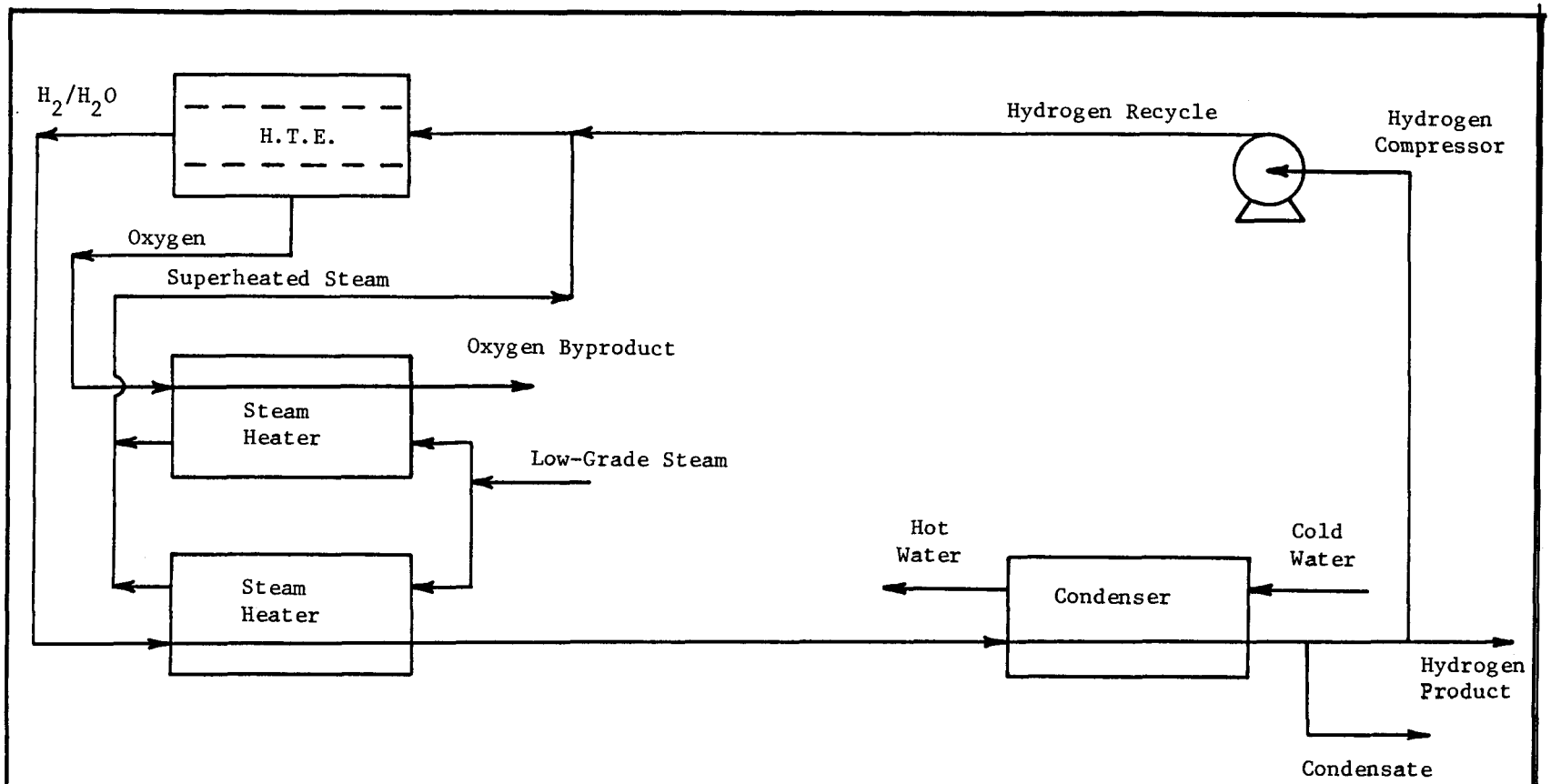

Process A: Steam Feed and Near-Isothermal H.T.E. Operation

MASSACHUSETTS INSTITUTE OF TECHNOLOGY SCHOOL OF CHEMICAL ENGINEERING PRACTICE	DATE 9-3-83	DRAWN BY MAL	FILE NO. MIT-BNL-83-3	FIG. 4-1

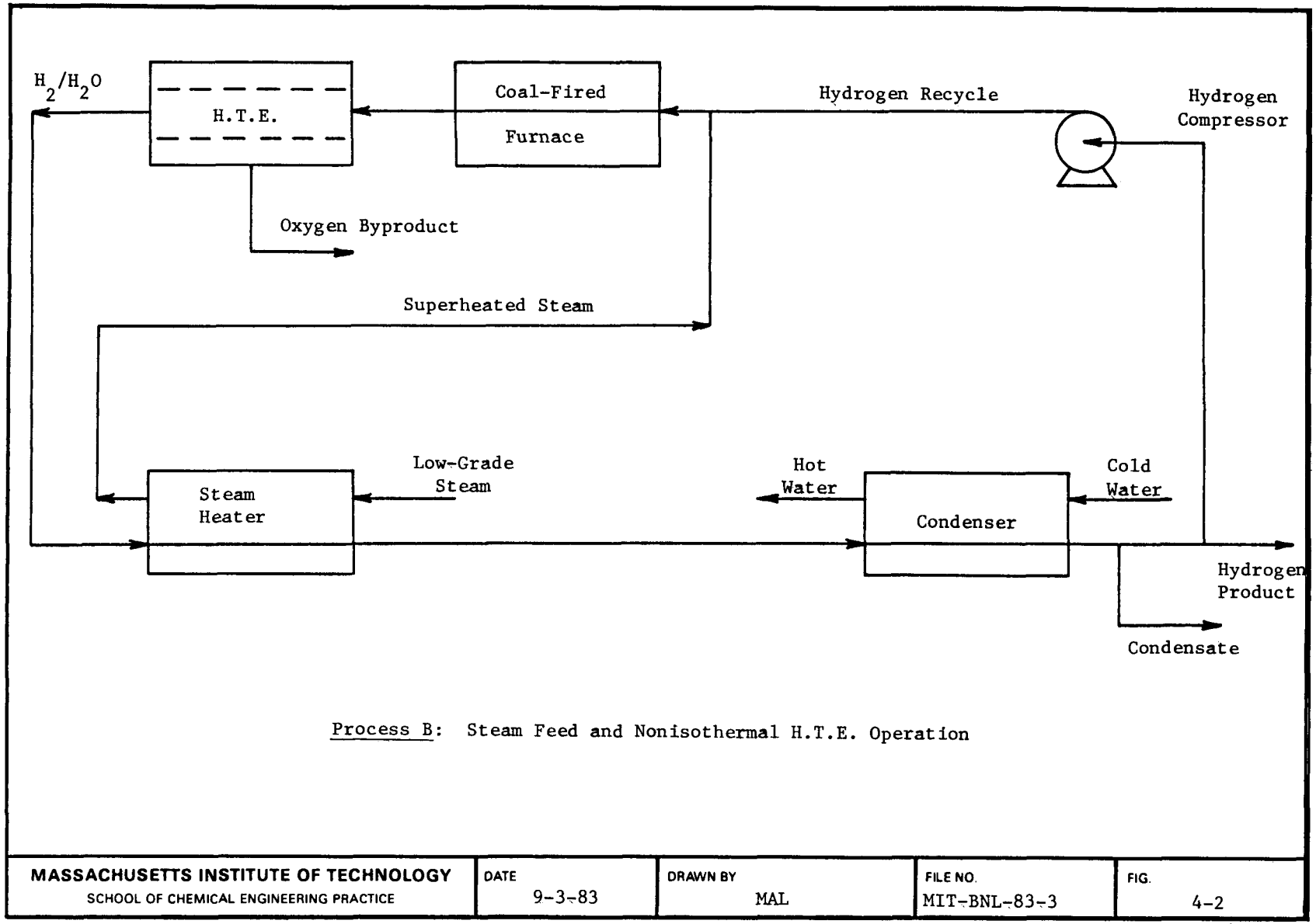

Process B: Steam Feed and Nonisothermal H.T.E. Operation

MASSACHUSETTS INSTITUTE OF TECHNOLOGY SCHOOL OF CHEMICAL ENGINEERING PRACTICE	DATE 9-3-83	DRAWN BY MAL	FILE NO. MIT-BNL-83-3	FIG. 4-2

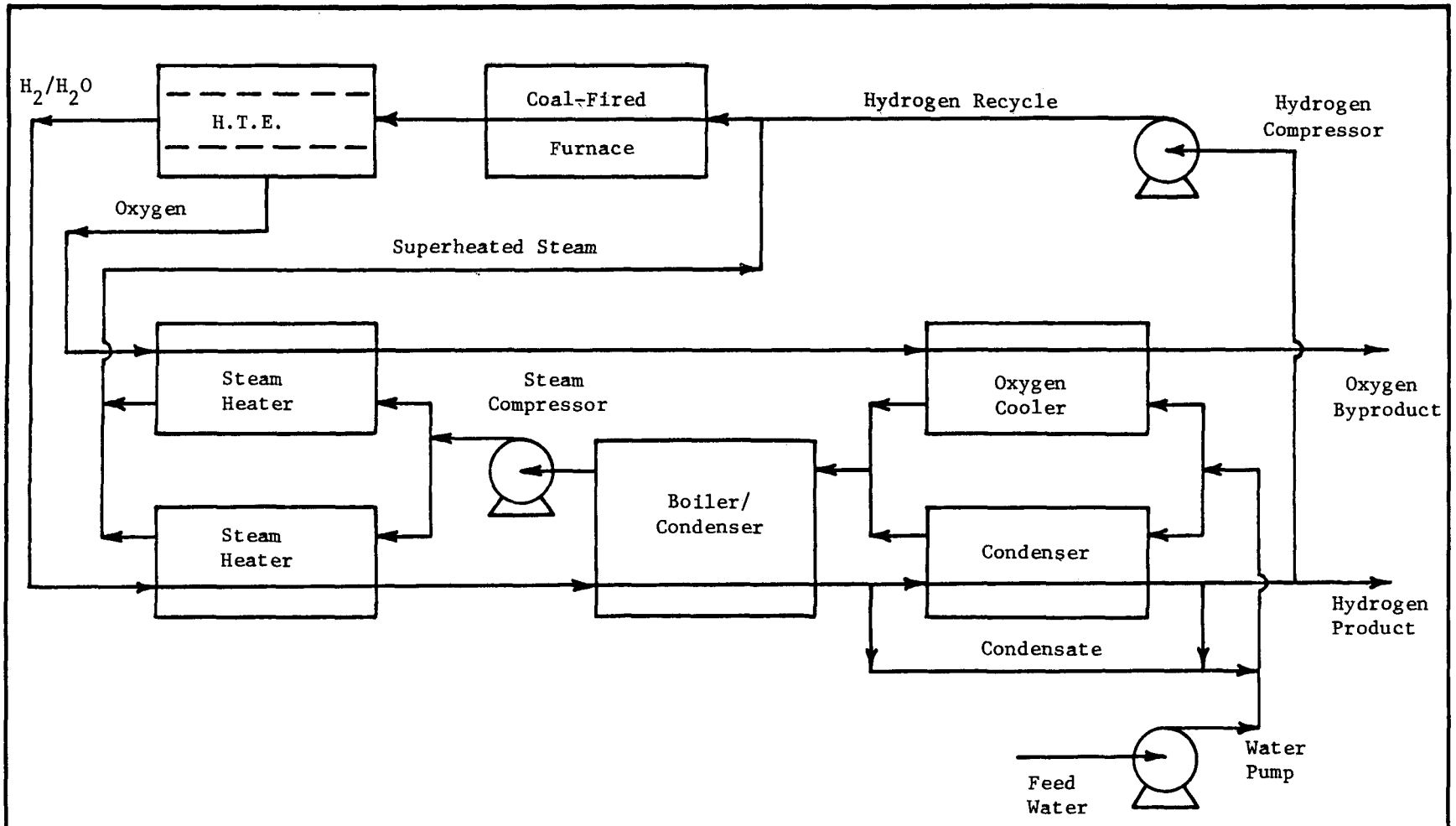

Process C: Water Feed and Nonisothermal H.T.E. Operation

MASSACHUSETTS INSTITUTE OF TECHNOLOGY SCHOOL OF CHEMICAL ENGINEERING PRACTICE	DATE 8-10-83	DRAWN BY MAL	FILE NO. MIT-BNL-83-3	FIG. 4-3

The final major process modification we considered is shown in Fig. (4-4). By allowing a 200°C temperature drop in each electrolyzer in a series and then reheating the gas stream before feeding to the next electrolyzer, the degree of substitution of electrical power input with thermal energy can be increased. The replacement of electrical energy with thermal energy can be maximized if only the electricity required for electrolysis is supplied to each of the electrolyzers. The steam conversion in each electrolyzer was found to be only 10% to 15%, but the overall conversion could exceed 90% with enough electrolyzers in series. The modification shown in Fig. (4-4) was applied to both Processes B and C. Because electrical power input is minimized, this modification gave a lower bound on hydrogen production cost and an upper bound on thermodynamic efficiency. A summary of the results obtained is given in Section 5.4.

4.2 Procedure for Technical and Economic Analysis of a Process Flowsheet

Consider the HTE process flowsheet shown in Fig. (4-5). Component mass flow rates and temperatures of each stream were determined by performing material and energy balances on each piece of equipment. The results for a 50% steam conversion are shown in Table (4-1). The ASPEN-PLUS process simulation program [Aspen Technology, Inc. (1983)] was used to calculate the values shown in this table, as described in Section 10.1. Hand calculations were also performed to verify the ASPEN-PLUS results. Good agreement (to within one percent of the computer-generated values) was obtained.

Table (4-1)
Material and Energy Balance Results for the HTE Process of Fig. (4-5) at a 50% Steam Conversion

Stream Number*	Mass Flow Rate (kg/sec) H_2	O_2	H_2O	Temperature (°C)
1	0	0	0.1186	153
2	0	0	1.1412	153
3	0	0	0.1186	1034
4	0	0	1.1412	1034
5	0.0074	0	1.2605	1000
6	0.0779	0	0.6303	1044
7	0	0.5597	0	1044
8	0.0779	0	0.6303	163
9	0	0.5597	0	648
10	0	0	0.6230	25
11	0.0074	0	0.0007	25
12	0.0074	0	0.0007	84
13	0.0705	0	0.0066	25
14	0	0	12.538	15
15	0	0	12.538	50

*As shown in Fig. (4-5)

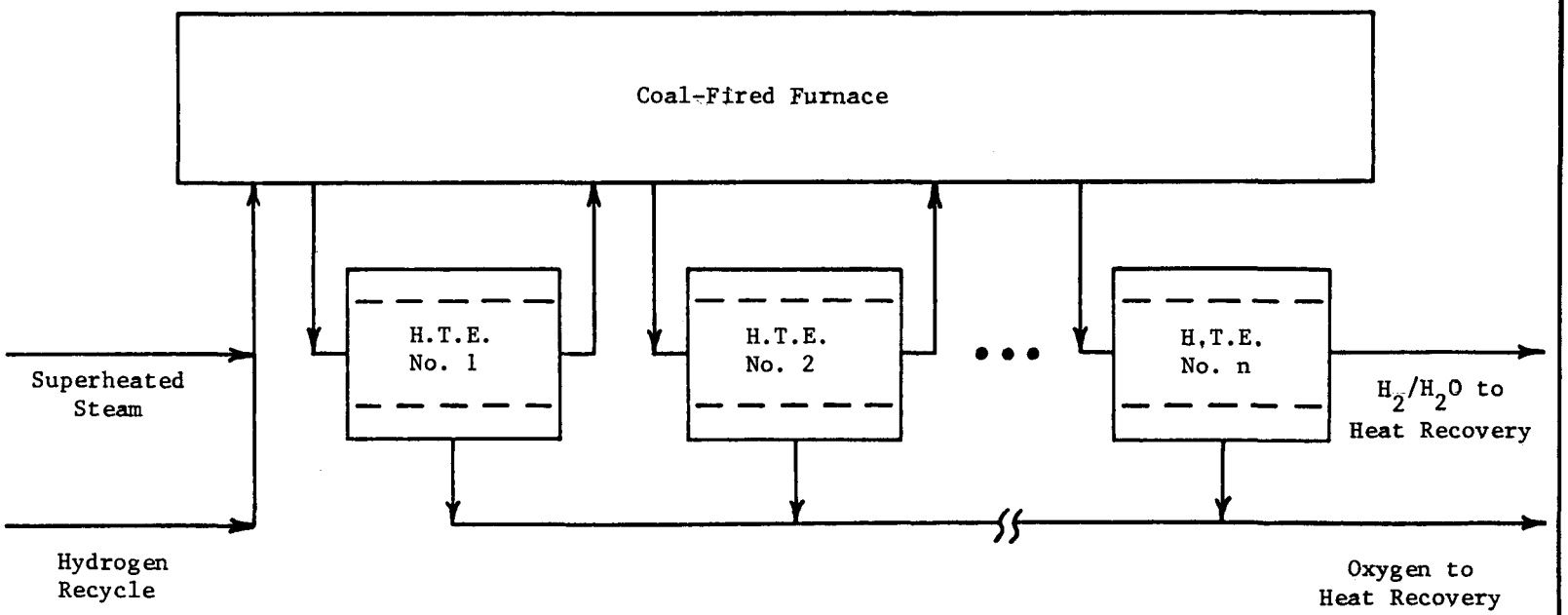

Reheating Between Staged Nonisothermal H.T.E.'s

MASSACHUSETTS INSTITUTE OF TECHNOLOGY SCHOOL OF CHEMICAL ENGINEERING PRACTICE	DATE 8-10-84	DRAWN BY MAL	FILE NO. MIT-BNL-83-3	FIG 4-4

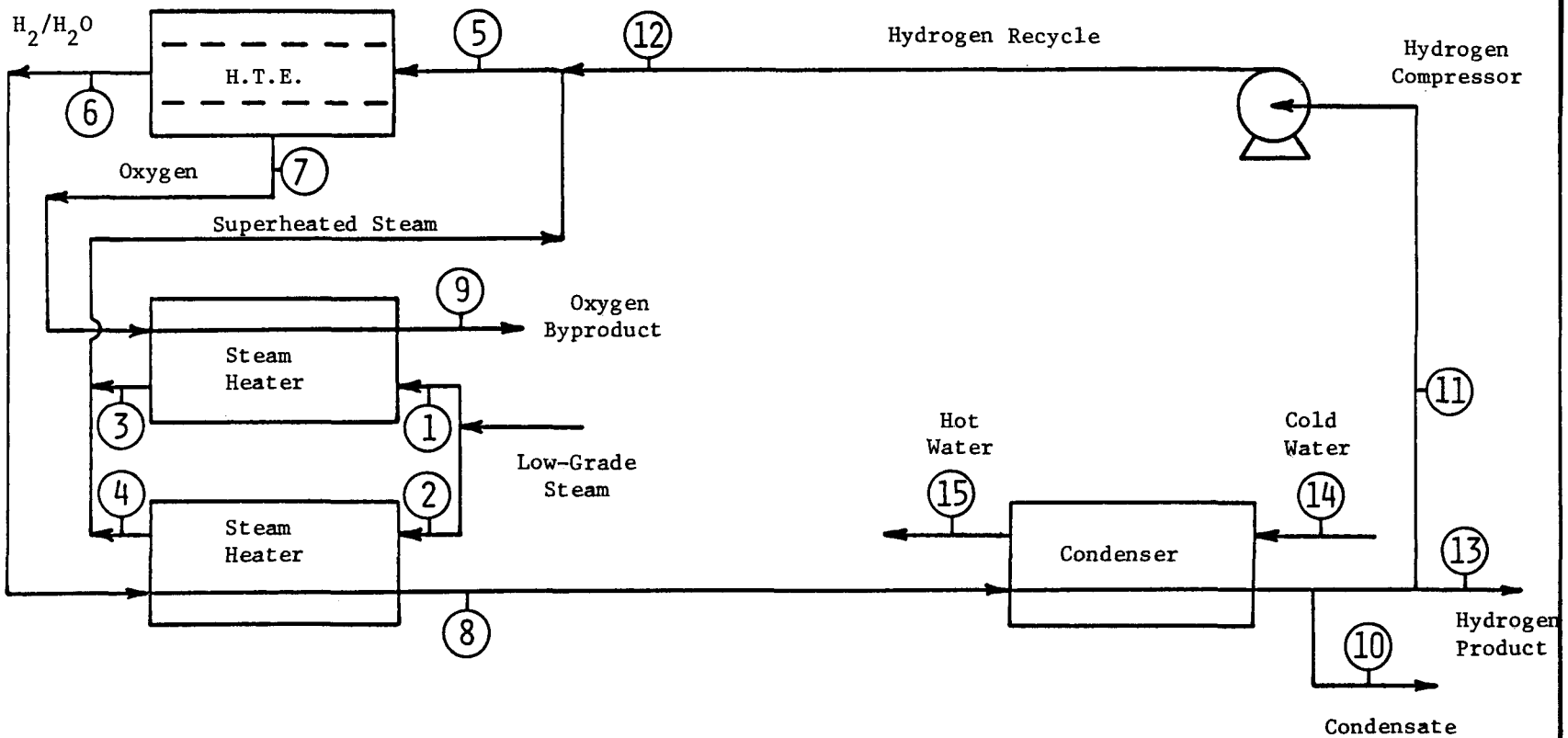

Example H.T.E. Process Flowsheet
[Stream numbers are referred to in Table (4-1)]

MASSACHUSETTS INSTITUTE OF TECHNOLOGY SCHOOL OF CHEMICAL ENGINEERING PRACTICE	DATE 9-3-83	DRAWN BY MAL	FILE NO. MIT-BNL-83-3	FIG. 4-5

Bavex heat exchangers were used for heat recovery in all of our process designs. These heat exchangers are fabricated with about 50% less material than an equivalent conventional shell-and-tube unit and their cost is approximately 40% of that of an equivalent shell-and-tube heat exchanger [DVT-USA (1983) and Kane (1983)]. The core of the Bavex exchanger is formed of metal sheets, ranging between 0.2 and 1 mm thick, that are stamped to impress a corrugated pattern in them. When two of these sheets are arranged back to back, a hollow "shell" is formed. When the shell assemblies are stacked, the rows of corrugations create "tubes." The material flow in the unit follows convoluted channels, thus creating turbulence and enhancing the Bavex exchanger's heat transfer capabilities. The Bavex exchanger can be fabricated from a wide range of materials including superalloys such as Inconel and Incoloy.

Heat transfer areas for the Bavex gas-gas heat exchangers were estimated from Eqs. (4-1) and (4-2) for a countercurrent heat exchanger (closely approximated by the Bavex exchanger) [Holman (1981)]:

$$A = \frac{Q}{U\ \Delta T_m} \quad , \tag{4-1}$$

where

$$\Delta T_m = \frac{(T_{h2} - T_{c1}) - (T_{h1} - T_{c2})}{\ln\left[\dfrac{(T_{h2} - T_{c1})}{(T_{h1} - T_{c2})}\right]} \quad . \tag{4-2}$$

The subscripts h and c refer to the hot and cold fluids, respectively, while the subscripts 1 and 2 refer to the heat exchanger inlet and outlet, respectively. Approximate values of overall heat transfer coefficients (U) were found in the literature [Holman (1981) and Perry and Chilton (1973)]. Heat exchanger costs were then estimated using average shell-and-tube heat exchanger cost data, in January 1979 dollars [Peters and Timmerhaus (1980)]. These costs were converted to 1983 dollars by multiplication with an inflation factor of 1.32 [Marshall and Swift (1983)].

The heat exchangers in a HTE process must operate at temperatures up to about 1000°C (1832°F), so they must be fabricated with materials having satisfactory high-temperature strength, such as high-nickel alloys. In addition, the heat exchangers with a steam-hydrogen mixture as the hot fluid must be made of alloys such as Monel, with good resistance against hydrogen embrittlement. The cost of these superalloy (high-nickel alloy) heat exchangers is about 3 to 5 times that of a comparably-sized carbon steel heat exchanger and about 1.5 to 3 times that of a stainless steel one [Peters and Timmerhaus (1980)]. Superalloy Bavex heat exchanger costs for the example considered are given in Table (4-2).

Preliminary estimates by Westinghouse suggest a high-temperature electrolyzer cost of about \$50/kW$_t$ H_2 produced [Fillo (1983)]. This cost estimate gave an electrolyzer cost of \$0.5 million for the assumed 10-MW$_t$ hydrogen production rate. The centrifugal hydrogen recycle compressor cost for this example was estimated at \$10,000, which resulted in a total purchased equipment cost of about \$1,280,000.

Table (4-2)
Heat Exchanger Costs for the HTE Process of Fig. (4-5)
at a 50% Steam Conversion

Heat Transfer Unit [as shown in Fig. (4-5)]	Heat Duty, Q (kW)	Overall Heat Transfer Coefficient, U (W/m^2 ^oC)	Heat Transfer Area, A (m^2)	Cost of Nickel-Alloy Bavex Heat Exchanger ($)
Oxygen Heat Exchanger	234	60	31	15,000
Steam-Hydrogen Exchanger	2252	60	3753	738,000
Condenser	1836	850*	43	17,000**

*The condenser was divided into two separate heat exchanger sections because the dew point of the steam-hydrogen mixture was 114°C, which was between the condenser inlet and outlet temperatures of this mixture [see Table (4-1)]. An overall heat transfer coefficient of 230 W/m^2 ^oC was assumed in the gas-water exchanger section of the condenser.

**The cost of a 316L stainless steel Bavex condenser of 43 m^2 would be about $10,000, while that of a 316L stainless steel shell-and-tube condenser would be about $25,000.

The total capital investment required for the process was estimated from the purchased equipment cost using the factored-estimate approach. Other expenses such as equipment installation, piping, instrumentation, insulation, and service facilities were included as specified fractions of the purchased equipment cost [Peters and Timmerhaus (1980)]. Table (4-3) gives a typical list of items considered and the cost associated with each one. The total capital cost is about four times the purchased equipment cost alone. The error in this kind of capital cost estimate is typically 30% [Peters and Timmerhaus (1980)], but, as shown in Section 5.1, this resulted in an error of only 6% in our HTE hydrogen production cost estimates. The hydrogen production cost error was low because electrical power cost accounted for about 80% of that production cost.

Table (4-3)
Breakdown of Capital Investment Components
for the HTE Process of Fig. (4-5) at a 50% Steam Conversion

Item	Cost
Purchased Equipment	$1,280,000
Equipment Installation	518,000
Insulation	116,000
Instrumentation and Control	259,000
Electrical Equipment	162,000
Buildings	155,000
Yard Improvements	194,000
Service Facilities	712,000
Land	78,000
Engineering	285,000
Construction	350,000
Contractor	168,000
Contingency	855,000
Total Capital Investment	$5,132,000

5 ANALYSIS OF ALTERNATIVE HIGH-TEMPERATURE STEAM ELECTROLYSIS FLOWSHEETS

This section summarizes our technical and economic analysis of the alternative high-temperature electrolysis (HTE) processes presented in the first part of Section 4. The first three parts of this section discuss HTE Processes A, B, and C. A foldout page showing the flowsheets for these processes is given at the end of Section 6. The last part of this section discusses modified versions of Processes B and C with reheating between staged nonisothermal electrolyzers.

5.1 Process A: Steam Feed and Isothermal High-Temperature Electrolyzer Operation

As shown in Fig. (6-3a) on the foldout page, there is no direct use of thermal energy in Process A. There is, therefore, no need to modify a coal-fired furnace by installing ceramic tubes for preheating the steam feed stream. Instead, more electrical energy must be supplied to the HTE than is needed for water-vapor electrolysis because the total endothermic heat of reaction is greater. This additional energy is dissipated by resistance heating and helps maintain near-isothermal conditions in the electrolyzer.

There was a temperature drop of 34°C (61°F) when the cold hydrogen recycle stream was mixed with the preheated steam. The temperature of the gas mixture must therefore rise 44°C (79°F) in the electrolyzer in order to have the assumed 10°C (18°F) approach at the hot end of each of the two steam-preheating exchangers (see Section 3.2 for design assumptions). As a result, the electrical energy input to the electrolyzer must be even more than that needed to maintain isothermality. Adding the hydrogen recycle stream before the preheaters would reduce this electrical energy input, but would result in larger, more expensive preheaters.

The total thermal energy content of the two electrolyzer product streams is greater than that needed to preheat the steam feed stream, without the hydrogen recycle, to a 10°C approach at the hot end of both heat exchangers (see Fig. (6-3a)). Heat exchanger operation could therefore range from a balanced steam-hydrogen exchanger and unbalanced oxygen exchanger to an unbalanced steam-hydrogen exchanger and balanced oxygen exchanger. A balanced heat exchanger would have a near-constant 10°C temperature difference along its length. The least expensive exchangers would both be unbalanced with cold end temperature differences greater than 10°C, but no effort was made to find this optimum. Instead, a balanced steam-hydrogen exchanger was chosen to maximize the heat duty of that exchanger and thereby minimize cooling water usage in the subsequent steam-hydrogen separating condenser. The temperature difference at the cold end of the oxygen exchanger then varied with steam conversion, ranging from 445°C (801°F) for a 90% conversion to 767°C (1381°F) for a 15% conversion.

For a 153°C (307°F) saturated steam feed and a 3 atm hydrogen product, the total capital cost estimated for Process A as a function of steam conversion in the electrolyzer is shown in Fig. (5-1). The electrolyzer cost

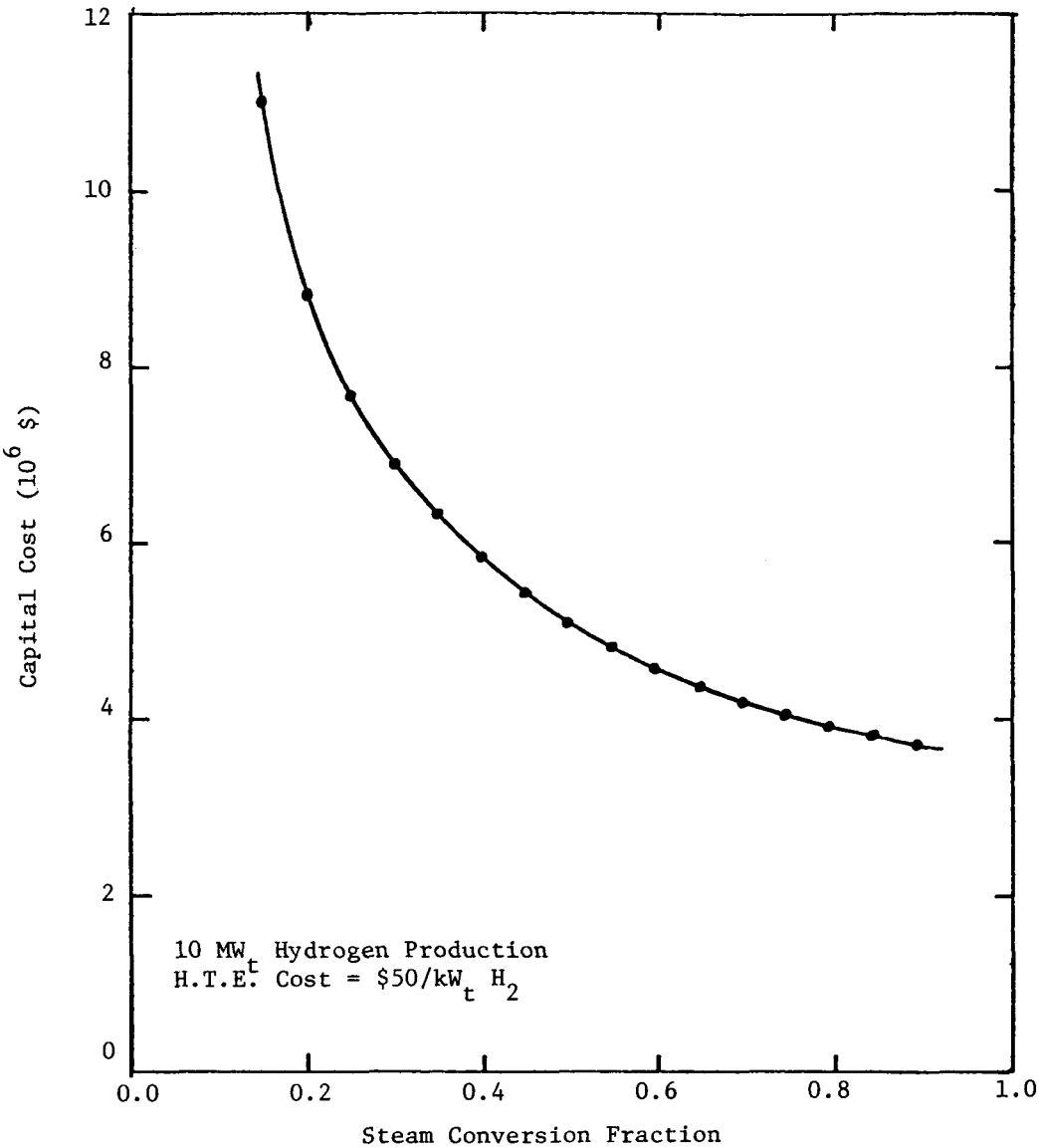

Capital Cost for Process A: Steam Feed and Near-Isothermal H.T.E. Operation

MASSACHUSETTS INSTITUTE OF TECHNOLOGY SCHOOL OF CHEMICAL ENGINEERING PRACTICE			
DATE 8-31-84	DRAWN BY AB	FILE NO MIT-BNL-83-3	FIG 5-1

assumed was \$0.5 million, or \$50/kW_t H_2 produced. As shown by the points in Fig. (5-1), costs were calculated at 5% steam conversion intervals. All of the figures in Section 5 are based on calculations at 5% conversion intervals.

A lower total capital cost would have been obtained if the total heat exchanger cost had been minimized. This minimization is especially desirable at low steam conversions, where heat exchangers account for up to 80% of the total purchased equipment cost. The lowest capital cost is obtained at high steam conversions because less feed steam must be processed.

Figure (5-2) shows the hydrogen production cost estimated for Process A as a function of steam conversion in the HTE. An electrical power cost of \$0.05/kWh was assumed, as well as a 20% annual capital recovery charge. As shown, electrical power makes up about 80% of the production cost and the capital recovery charge only becomes important at low steam conversions. A steam cost of 0.69¢/kg (\$3.10/1000 lbm) is an upper bound [Peters and Timmerhaus (1980)], so the steam cost is also not very important except at low steam conversions.

The thermodynamic efficiency of Process A with respect to the primary energy source (thermal energy from coal) is plotted as a function of steam conversion in Fig. (5-3). Thermodynamic efficiencies of 35% for electrical power generation and 100% for steam generation were assumed. The efficiency is poor at low steam conversions because almost all of the unconverted steam is condensed, with the accompanying loss of the thermal energy used to generate that steam. Feeding higher-pressure saturated steam to the process at a correspondingly higher temperature gives lower thermodynamic efficiencies because even more thermal energy is lost to the cooling water in the condenser.

For near-isothermal electrolyzer operation, minimum capital and operating costs are both obtained at high steam conversions. This gives a minimum production cost at high conversions of \$0.19 to \$0.20/m^3 H_2 produced (\$16 to \$17/10^6 Btu). As an added benefit, thermodynamic efficiency from coal-fired heat is also a maximum at high steam conversions.

5.2 Process B: Steam Feed and Nonisothermal High-Temperature Electrolyzer Operation

The second process flowsheet which we considered, Process B, is shown in Fig. (6-3b) on the foldout page. Process B is similar to Process A, which was considered in the preceding part of this section, except that a coal-fired furnace has been fitted with ceramic tubes to preheat the electrolyzer feed stream to 1100°C (2012°F). This extra heat supplied by the furnace permits a temperature drop of 200°C (360°F) from the inlet to the outlet of the HTE, while still maintaining a 1000°C (1832°F) average operating temperature. In this way less expensive thermal energy (\$2/10^6 Btu) is substituted for electrical energy (\$0.05/kWh).

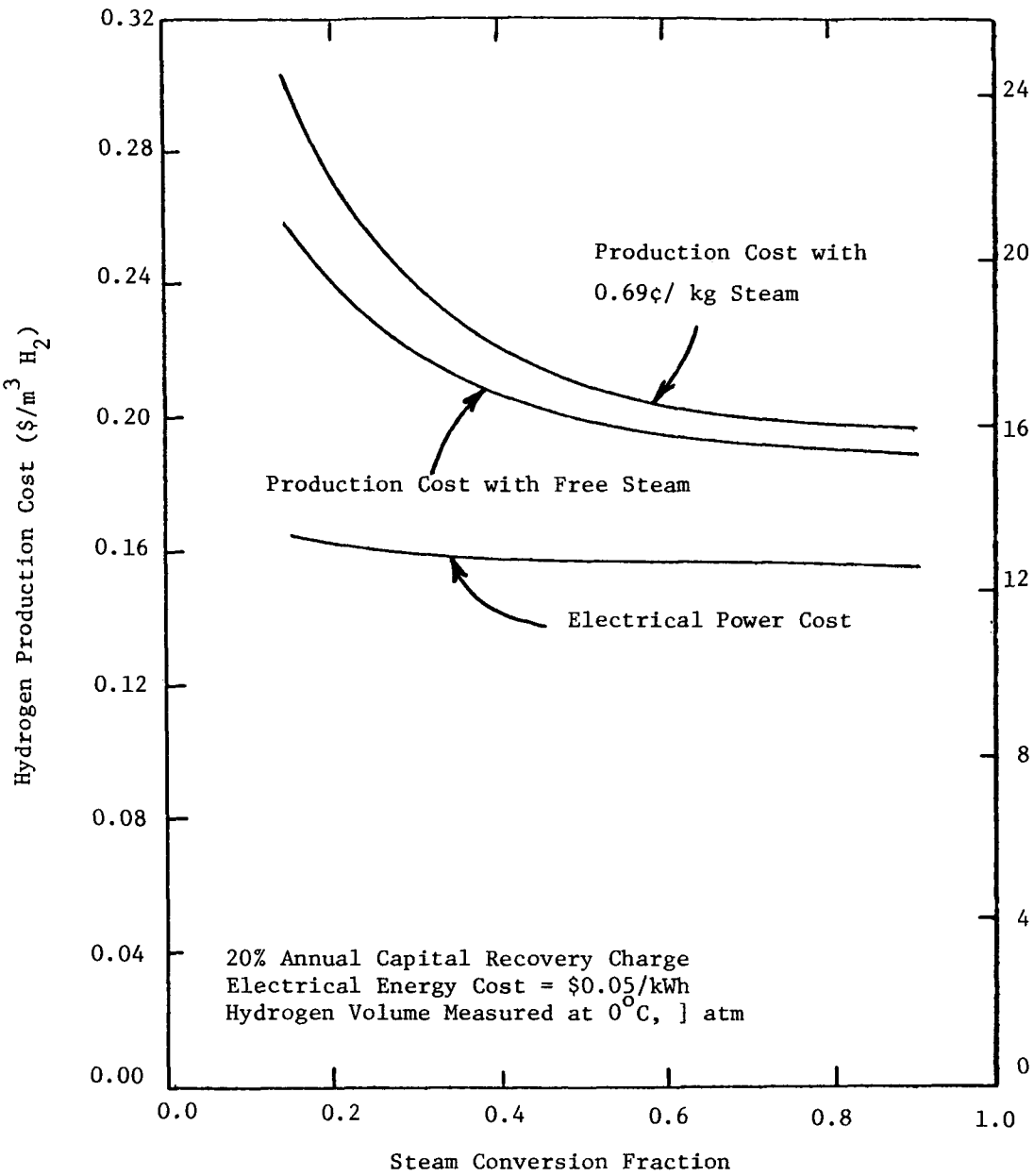

Hydrogen Production Cost for Process A: Steam Feed and Near-Isothermal H.T.E. Operation

MASSACHUSETTS INSTITUTE OF TECHNOLOGY SCHOOL OF CHEMICAL ENGINEERING PRACTICE			
DATE 8-31-83	DRAWN BY AB	FILE NO MIT-BNL-83-3	FIG 5-2

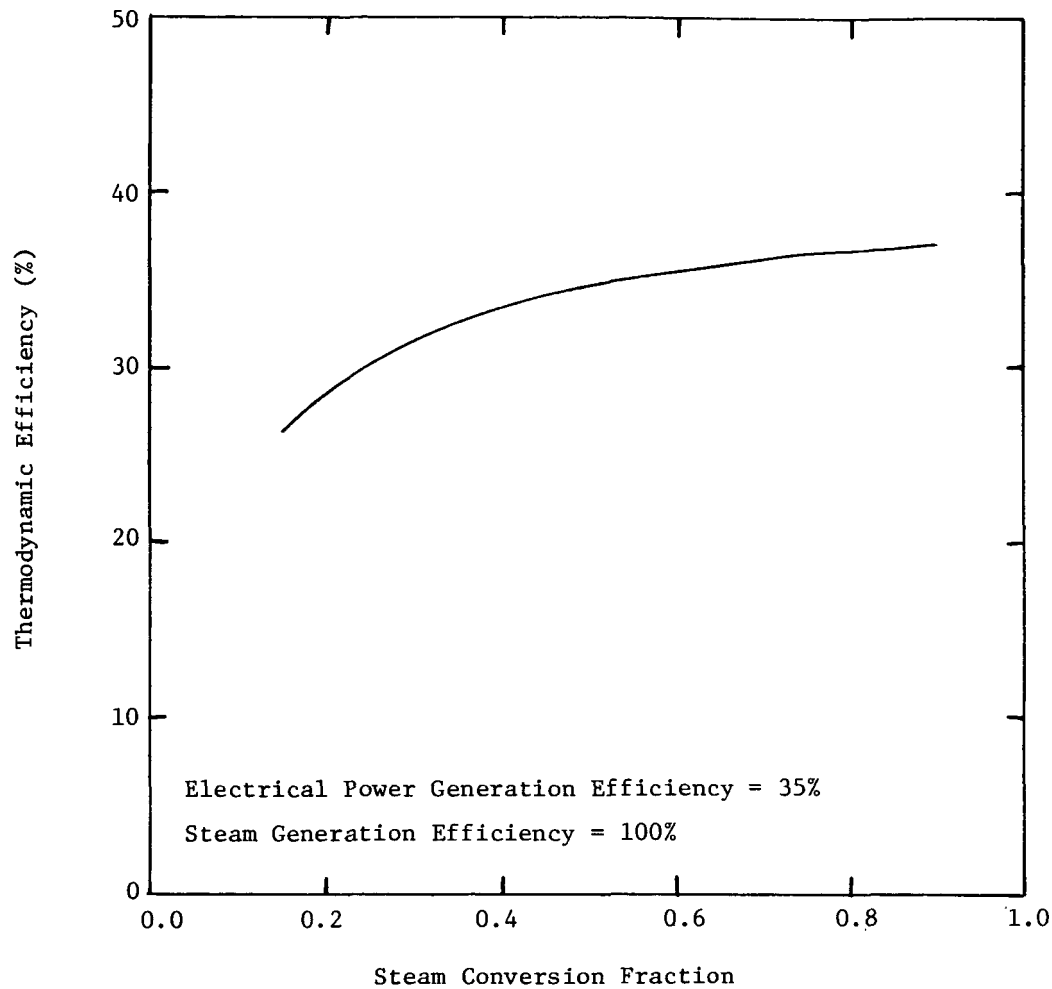

Thermodynamic Efficiency for Process A: Steam Feed and Near-Isothermal H.T.E. Operation

MASSACHUSETTS INSTITUTE OF TECHNOLOGY SCHOOL OF CHEMICAL ENGINEERING PRACTICE			
DATE 8-31-84	DRAWN BY AB	FILE NO MIT-BNL-83-3	FIG 5-3

In addition, the enthalpy of the oxygen product stream is not recovered, eliminating one steam-preheating exchanger. This also makes the steam-hydrogen exchanger smaller because, unlike in Process A, it is no longer a balanced exchanger. The temperature difference at the cold end was still 10°C (18°F), while the difference at the hot end varied from 17°C (31°F) for a 15% steam conversion to 145°C (261°F) for a 90% conversion.

Eliminating the oxygen heat exchanger increased the heat duty required in the furnace by up to about 0.2 MW_t (0.7 x 10^6 Btu/hr) but also reduced capital cost. This elimination would be less economically attractive in Process A, where the lost heat recovery must be replaced by electrical resistance heating in the electrolyzer. The total capital cost for Process B is lower at all steam conversions than that shown in Fig. (5-1) for Process A.

Figure (5-4) shows the hydrogen production cost estimated for Process B as a function of steam conversion in the HTE. As before, an electrical power cost of $0.05/kWh and 20% annual capital recovery charge have been assumed. The cost of coal-fired heat was assumed to be $2/$10^6$ Btu. The electrical power cost for Process A is shown as a dotted line. The electrical power cost for Process B is lower than that for Process A because some thermal energy has been substituted for electrical power. The fraction of thermal energy substituted is greater at lower steam conversions, where the electrolyzer feed stream has a higher initial enthalpy content.

The total hydrogen production cost was lower for Process B than for Process A because of the reduced electrical power cost. The production cost for Process B was as low as $0.17 to $0.18/$m^3$ H_2 produced ($14 to $15/$10^6$ Btu) for steam conversions greater than 50%. The thermodynamic efficiency was also higher for Process B than for Process A, as shown in Fig. (5-5), because less electrical power generated at a 35% conversion efficiency is used.

For Process B, we also found that replacing heat recovery capacity with additional preheat duty in the coal-fired furnace actually reduced production cost. This reduction occurred because the decrease in capital recovery cost with smaller heat exchangers was greater than the increase in thermal energy cost for additional coal. Reducing heat recovery capacity also decreased the thermodynamic efficiency of Process B, however. This effect is shown in Table (5-1) for 30% and 90% steam conversions in the electrolyzer. Completely eliminating heat recovery has the greatest effect on efficiency at low conversions, where the steam feed rate and preheat duty are high.

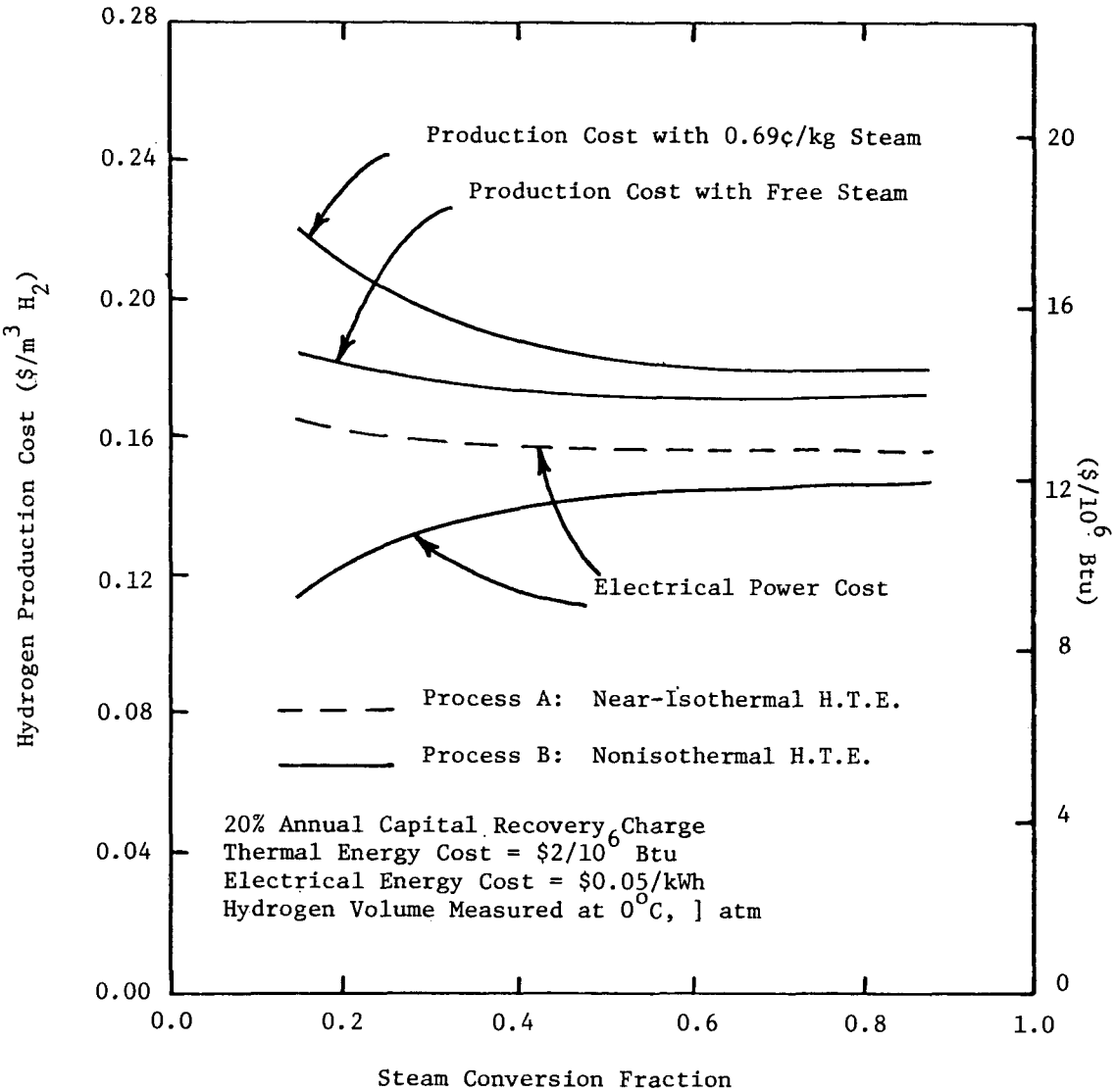

Hydrogen Production Cost for Process B: Steam Feed and Nonisothermal H.T.E. Operation

MASSACHUSETTS INSTITUTE OF TECHNOLOGY SCHOOL OF CHEMICAL ENGINEERING PRACTICE			
DATE 8-31-83	DRAWN BY AB	FILE NO MIT-BNL-83-3	FIG. 5-4

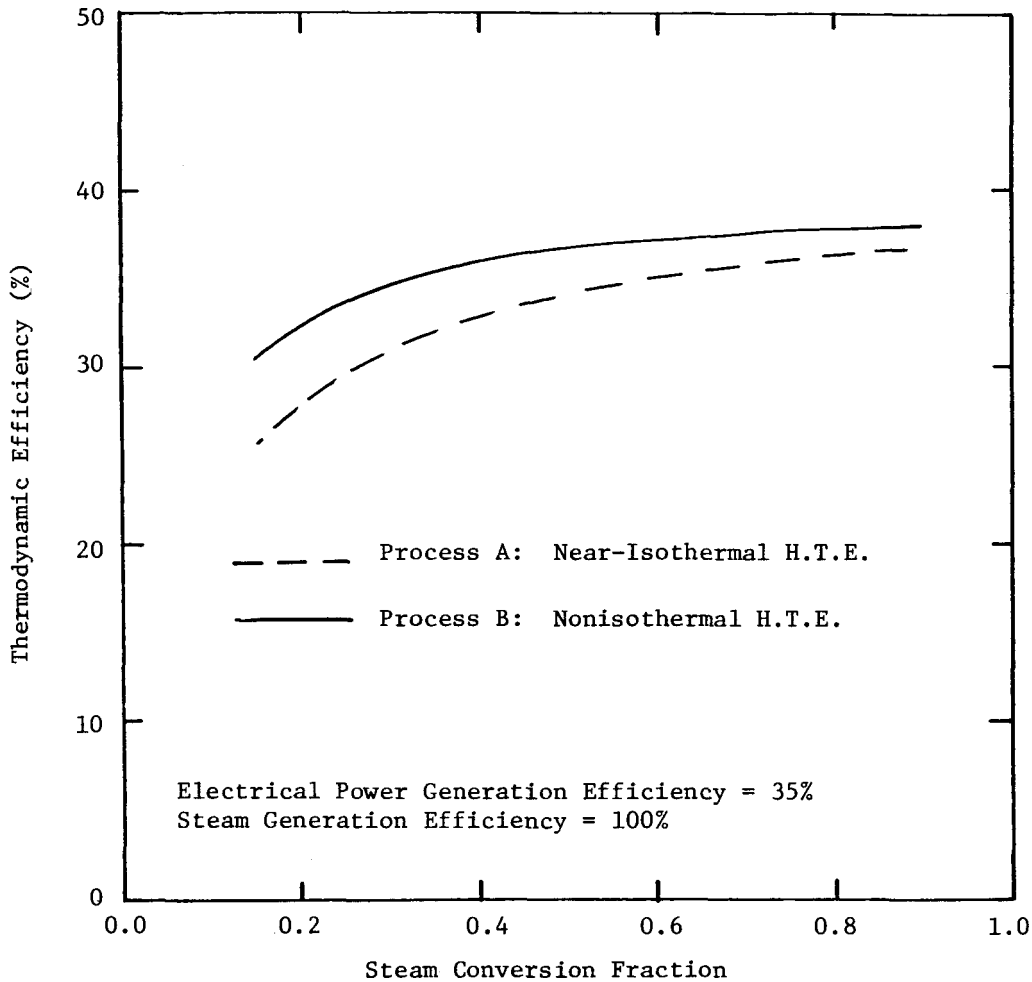

Comparison of Thermodynamic Efficiencies for Processes A and B: Steam Feed

MASSACHUSETTS INSTITUTE OF TECHNOLOGY SCHOOL OF CHEMICAL ENGINEERING PRACTICE			
DATE 8-31-83	DRAWN BY AB	FILE NO MIT-BNL-83-3	FIG 5-5

Table (5-1)
Effect of Heat Recovery on the Thermodynamic Efficiency of Process B: Steam Feed and Nonisothermal HTE Operation

Process	Steam Conversion Fraction	Thermodynamic Efficiency (%)
Process B, as shown in Fig. (6-3b)	0.30	34.7
	0.90	38.2
Process B, without Steam-Hydrogen Heat Recovery	0.30	31.1
	0.90	36.6

5.3 Process C: Water Feed and Nonisothermal High-Temperature Electrolyzer Operation

The third process flowsheet which we considered, Process C, is shown in Fig. (6-3c) on the foldout page. Rather than feeding saturated steam to the system, the enthalpy of the product streams is used to boil liquid water within the process. As in Process B, the electrolyzer operates with a 200°C (360°F) temperature drop and coal-fired heat is used to preheat the electrolyzer feed stream to 1100°C (2012°F).

In order to generate steam internally, the pressure of the steam-hydrogen product stream must be higher than that of the feed water so that its condensing temperature range will also be higher than the boiling temperature of the feed water. The pressure difference must be increased in order to operate at high electrolyzer steam conversions because the dew point of the steam-hydrogen product mixture decreases as the steam mole fraction decreases unless the total product pressure is increased. When boiling water at 1 atm, steam conversions up to about 35% can be achieved for a hydrogen product pressure of 3 atm. This upper limit increases to about 55% for a hydrogen product pressure of 10 atm. A centrifugal compressor having an efficiency of 70% with respect to isentropic compression was used to increase the pressure of the saturated steam leaving the boiler.

In analyzing Process C, we found that the location of pinch points in the heat exchangers shown in Fig. (6-3c) shifted with changes in steam conversion and in the pressure difference between the feed water and hydrogen product. This made modeling the flowsheet with the ASPEN-PLUS simulator program difficult because a modified list of input instructions was required for each new set of exchanger pinch points. As the pinch points shifted, heat recovery in the low-temperature oxygen byproduct cooler sometimes became unnecessary, while at high steam conversions an additional water-cooled exchanger was required to reduce the hydrogen product temperature to 25°C (77°F).

Figure (5-6) shows the hydrogen production cost estimated for this process as a function of steam conversion in the HTE. An electrical power cost of \$0.05/kWh, coal-fired heat cost of $\$2/10^6$ Btu, and 20% annual capital recovery charge have again been assumed. The electrical power cost is higher for Process C than for Process B because of the addition of a steam compressor. This effect is greatest at low steam conversions, where the steam generation rate is higher.

The total production cost is about 10% greater for Process C than for Process B, primarily because of the steam compression cost. However, the thermodynamic efficiency is higher for the same steam conversion because of greater heat recovery. For example, the thermodynamic efficiency of Process B is 34.7% for a 30% steam conversion in the electrolyzer, while that of Process C is 38.5%. Use of higher product pressures reduces efficiency because more electrical power is needed for steam compression (see Fig. (5-7)).

Steam compression cost can be reduced by recycling the steam-hydrogen mixture at 900°C (1652°F) rather than the hydrogen product at 25°C in order to have 5 mol % hydrogen at the HTE inlet. A scheme to do this is shown in Fig. (5-8). A suction pump, or gas ejector, is used to mix the recycle steam-hydrogen stream with newly generated steam having a higher pressure than that stream. The reduction in hydrogen production cost was only about 1% for a 35% steam conversion in the HTE, but the savings would be higher at lower conversions.

5.4 Processes with Reheating between Staged Nonisothermal High-Temperature Electrolyzers

By introducing reheating between staged nonisothermal electrolyzers as shown in Fig. (4-4), the amount of electrolysis energy supplied thermally can be increased. The amount of this increase is limited by thermodynamic considerations, however. Under isothermal conditions, the theoretical (reversible) cell potential is given by

$$E = \frac{\Delta G}{nF} \quad . \tag{5-1}$$

Real electrolysis cells have an even higher potential due to irreversibilities such as internal resistance and overpotentials.

To estimate the actual minimum electrical input possible in HTE cells, we analyzed data obtained at 1000°C (1832°F) by Westinghouse [Isenberg (1981)]. These data have been used in the plots of actual electrolysis cell potential (E') as a function of hydrogen mole fraction in the gas phase (x) which are shown in Fig. (5-9).

For electrolysis cells in series, the total electrical power required is

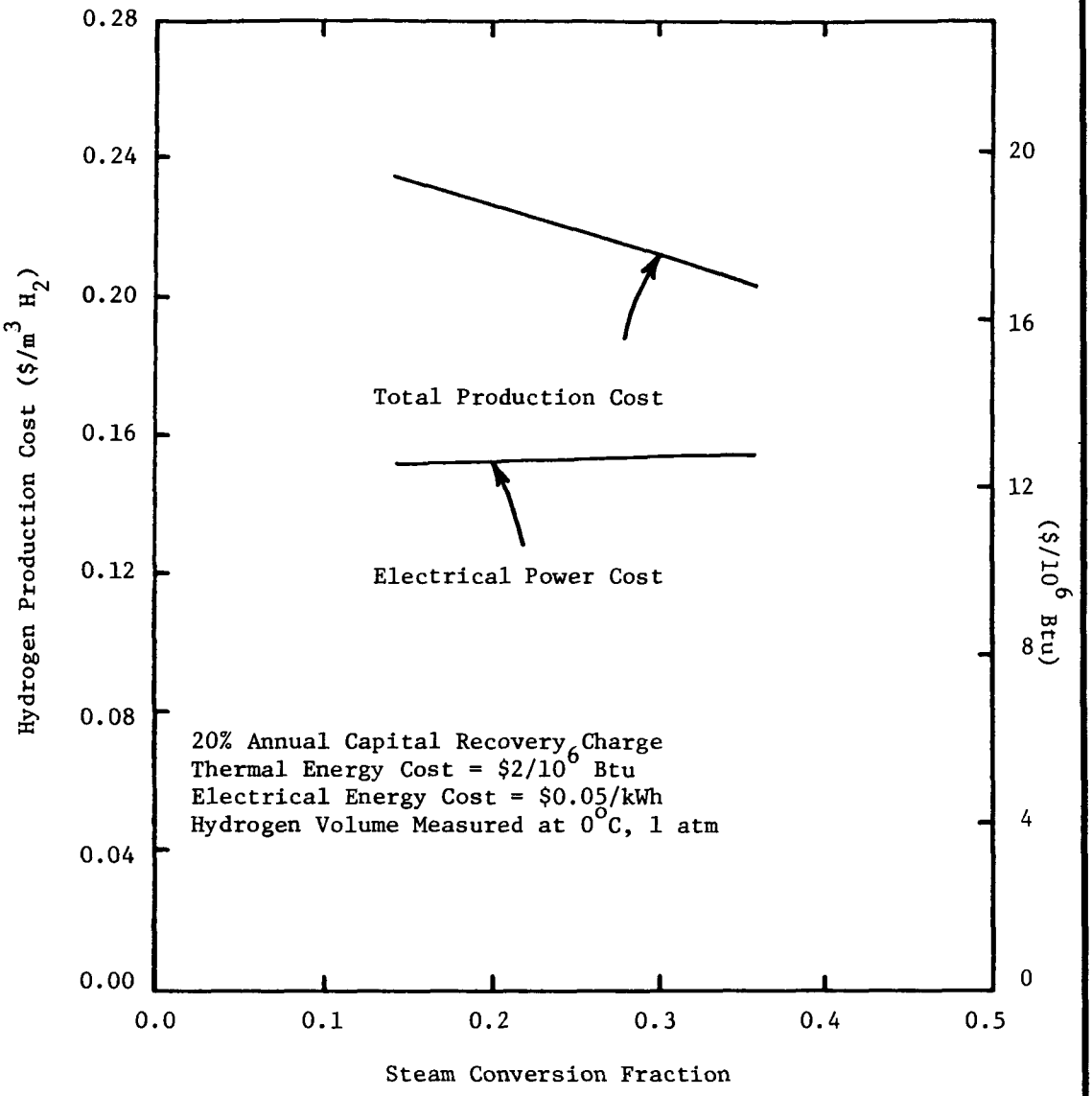

Hydrogen Production Cost for Process C: Water Feed and Nonisothermal H.T.E.

MASSACHUSETTS INSTITUTE OF TECHNOLOGY SCHOOL OF CHEMICAL ENGINEERING PRACTICE			
DATE 8-31-83	DRAWN BY AB	FILE NO MIT-BNL-83-3	FIG 5-6

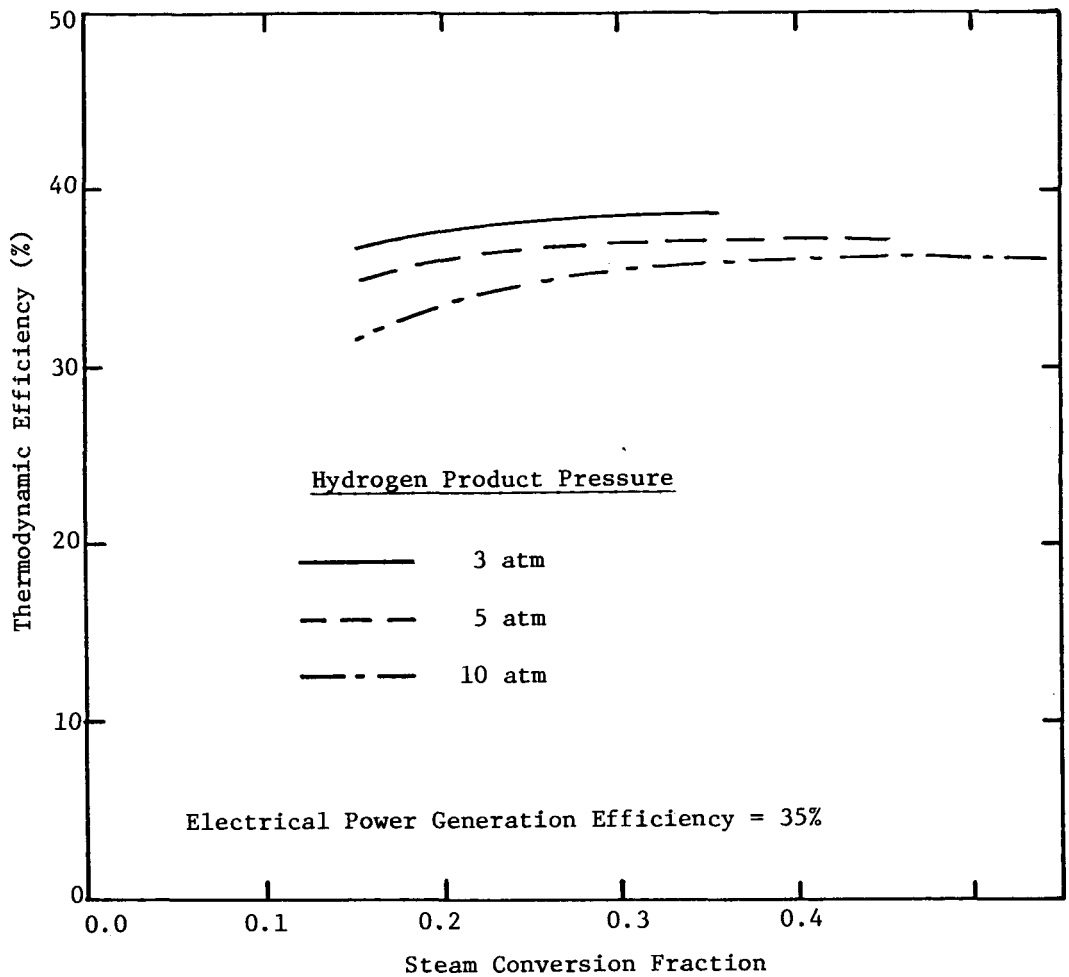

Thermodynamic Efficiency for Process C: Water Feed and Nonisothermal H.T.E. Operation

MASSACHUSETTS INSTITUTE OF TECHNOLOGY SCHOOL OF CHEMICAL ENGINEERING PRACTICE			
DATE 8-31-83	DRAWN BY AB	FILE NO MIT-BNL-83-3	FIG 5-7

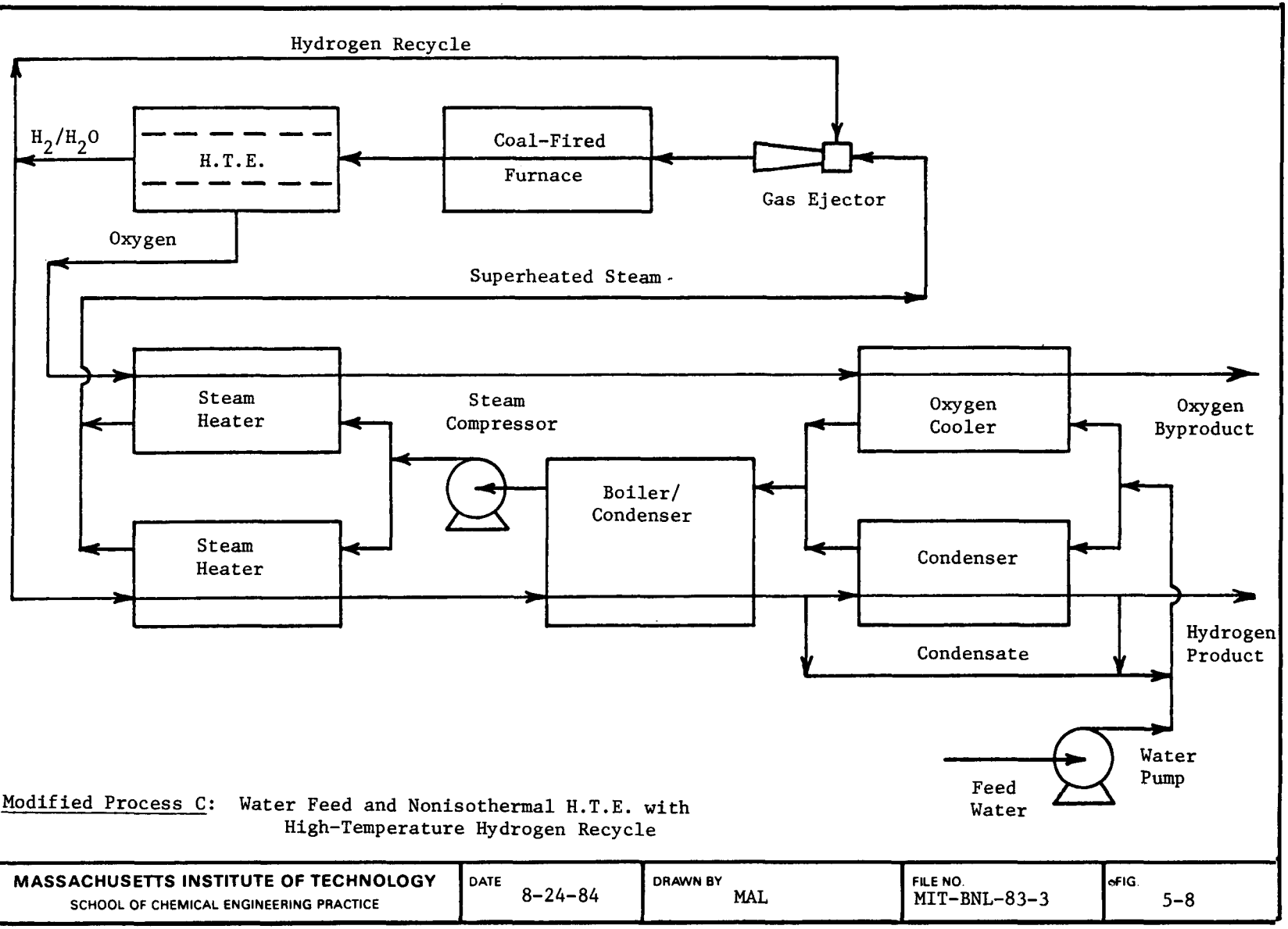

Modified Process C: Water Feed and Nonisothermal H.T.E. with High-Temperature Hydrogen Recycle

MASSACHUSETTS INSTITUTE OF TECHNOLOGY SCHOOL OF CHEMICAL ENGINEERING PRACTICE	DATE 8-24-84	DRAWN BY MAL	FILE NO. MIT-BNL-83-3	FIG. 5-8

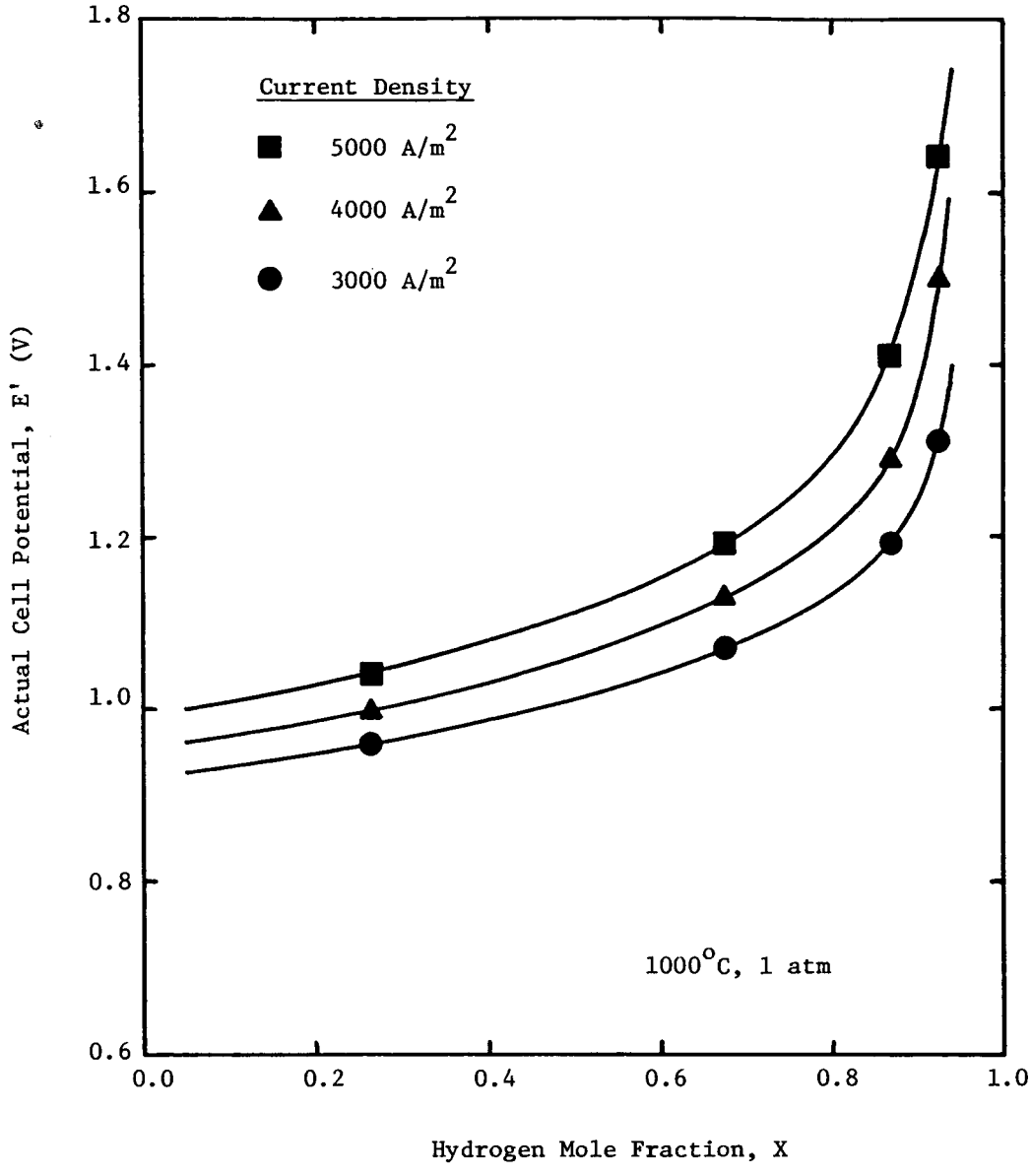

Actual Westinghouse H.T.E. Cell Potential as a Function of Hydrogen Concentration in the Cell

MASSACHUSETTS INSTITUTE OF TECHNOLOGY SCHOOL OF CHEMICAL ENGINEERING PRACTICE			
DATE 9-5-83	DRAWN BY MAL	FILE NO MIT-BNL-83-3	FIG 5-9

$$W = - nF \sum_{i=1}^{N} E_i' \Delta m_i \qquad (5\text{-}2)$$

The change in steam flow rate is related to hydrogen mole fraction by

$$\Delta m = \frac{- m_o}{1 - x_o} \Delta x \quad , \qquad (5\text{-}3)$$

where the subscript o refers to the inlet values. For small Δx and x_o = 0.05, Eq. (5-2) can be approximated by

$$W = nF \frac{m_o}{0.95} \int_{0.05}^{x} E' \, dx \quad . \qquad (5\text{-}4)$$

The outlet hydrogen mole fraction can in turn be related to the steam conversion. The value of Eq. (5-4) as a function of steam conversion is given as a solid line in Fig. (5-10) for a current density of 5000 A/m^2 (465 A/ft^2) and hydrogen production rate of 10 MW_t. Note that even at 90% steam conversion the electrolysis cell power input is less than that required to maintain isothermal operation (dotted line).

The curve of electrolysis power vs. steam conversion in Fig. (5-10) was used to estimate the reduction in hydrogen production cost as a function of the number of nonisothermal HTE's in series for Processes B and C (Figs. (6-3b) and (6-3c) on the foldout page). The results obtained for Process C (the water-fed case) are shown in Fig. (5-11). For a fixed current density of 5000 A/m^2 and temperature drop of 200°C (360°F), the overall steam conversion increases by 10% to 15% in each electrolyzer (solid dots). The solid line represents a single electrolyzer with a 200°C temperature drop. The point for two HTE's in series has been corrected down to this line because operation with two electrolyzers at a 5000 A/m^2 current density was actually more expensive than the single electrolyzer. The hydrogen production cost reduction for three or more electrolyzers in series was \$0.01 to \$0.02/m^3 H_2 produced (\$0.8 to \$2/10^6 Btu) in both Processes B and C. This represents a 5% to 10% savings.

We did not examine process operation with interstage reheating in great detail. Actual design of such a system would have to deal with the potential problems involved in running ceramic tubes back and forth between a coal-fired furnace and the electrolyzers. Heat losses would be an important consideration, as would be the added pressure drop required for flow through the interstage piping.

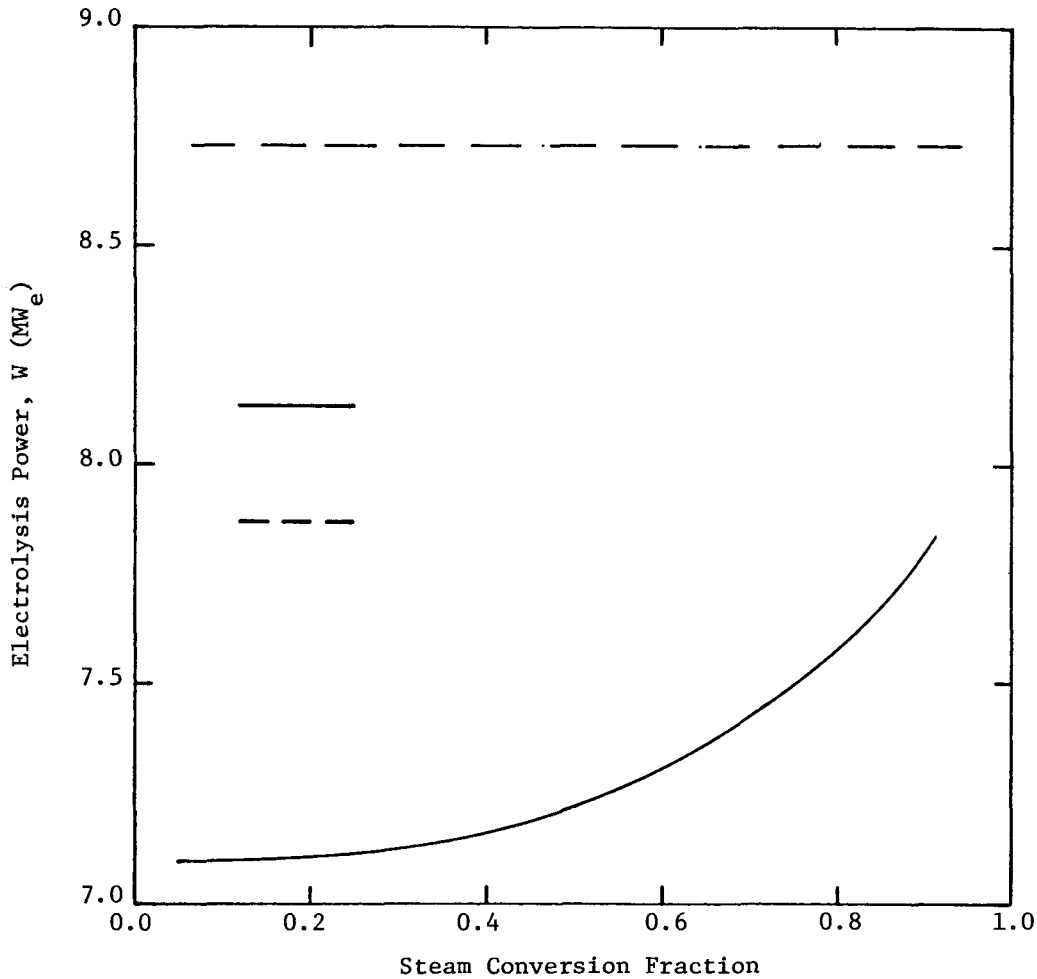

Electrolysis Power Requirements for 10 MW_t Hydrogen Production

MASSACHUSETTS INSTITUTE OF TECHNOLOGY SCHOOL OF CHEMICAL ENGINEERING PRACTICE			
DATE 8-31-83	DRAWN BY AB	FILE NO. MIT-BNL-83-3	FIG 5-10

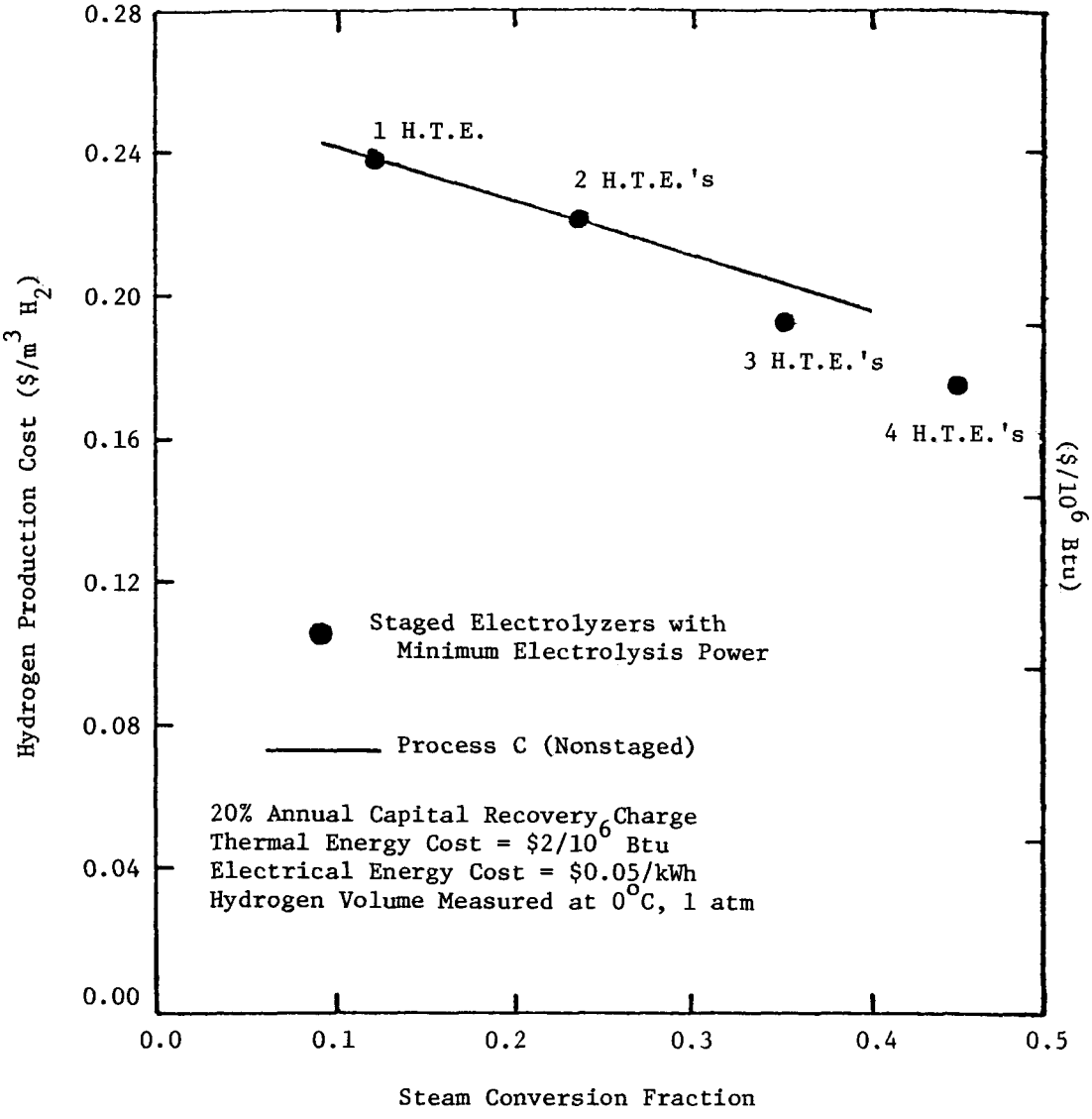

Comparison of Hydrogen Production Costs for Staged and Nonstaged Processes: Water Feed and Nonisothermal H.T.E. Operation

MASSACHUSETTS INSTITUTE OF TECHNOLOGY SCHOOL OF CHEMICAL ENGINEERING PRACTICE			
DATE 8-31-83	DRAWN BY AB	FILE NO MIT-BNL-83-3	FIG 5-11

6 COMPARISON OF ALTERNATIVE HYDROGEN PRODUCTION PROCESSES

The first part of this section compares the hydrogen production costs we estimated for each of the alternative high-temperature water-vapor electrolysis (HTE) processes discussed in Section 5. A foldout page showing the flowsheets for processes A, B, and C is given at the end of this section. The second part of this section gives a brief comparison of HTE hydrogen production costs with those for competing hydrogen production processes.

6.1 Comparison of Alternative High-Temperature Steam Electrolysis Process Flowsheets

Before comparing the HTE hydrogen production processes we studied, this section presents a short discussion on the sensitivity of our hydrogen production cost estimates to the two primary components of those estimates: annual capital recovery charge and electrical power cost. Consideration of the capital recovery charge is important since the actual cost and reliability of commercial HTE units is not yet known. The cost of electricity is considered because it was the major component of HTE hydrogen production cost.

Figure (6-1) shows hydrogen production cost for the water-fed process (Process C) with staged nonisothermal electrolyzers as a function of electrolyzer cost for several annual capital recovery charges and a 35% steam conversion. In this figure, the cost of electrical power was taken as \$0.05/kWh and that of thermal energy as $\$2/10^6$ Btu. The volume of the hydrogen product has been calculated at 0^oC (32^oF) and 1 atm here and in the following discussion. Preliminary estimates by Westinghouse have predicted a high-temperature electrolyzer cost of about $\$50/kW_t$ H_2 produced [Fillo (1983)]. At this cost, the assumed annual capital recovery charge does not affect the hydrogen production cost significantly. The hydrogen production cost increases more rapidly with increasing electrolyzer cost for higher annual capital recovery charges. The hydrogen production cost behaves similarly as a function of electrolyzer cost and annual capital recovery charge for the other processes we considered.

The hydrogen production cost for a 35% steam conversion is given as a function of electrical power cost in Fig. (6-2). An electrolyzer cost of $\$50/kW_t$ H_2, thermal energy cost of $\$2/10^6$ Btu, and 20% annual capital recovery charge have been assumed. The hydrogen production cost is strongly dependent on the cost of electrical power for all of the processes considered. For a water-fed process with isothermal HTE operation, a \$0.01/kWh increase in electrical power cost results in a $\$0.03/m^3$ H_2 ($\$2/10^6$ Btu) increase in hydrogen production cost, which represents an increase of about 15%. The other processes we considered exhibited similar increases in hydrogen production cost with increasing electrical power cost (see Fig. (6-2)). This behavior is to be expected since electrical power cost was the major component of HTE hydrogen production cost.

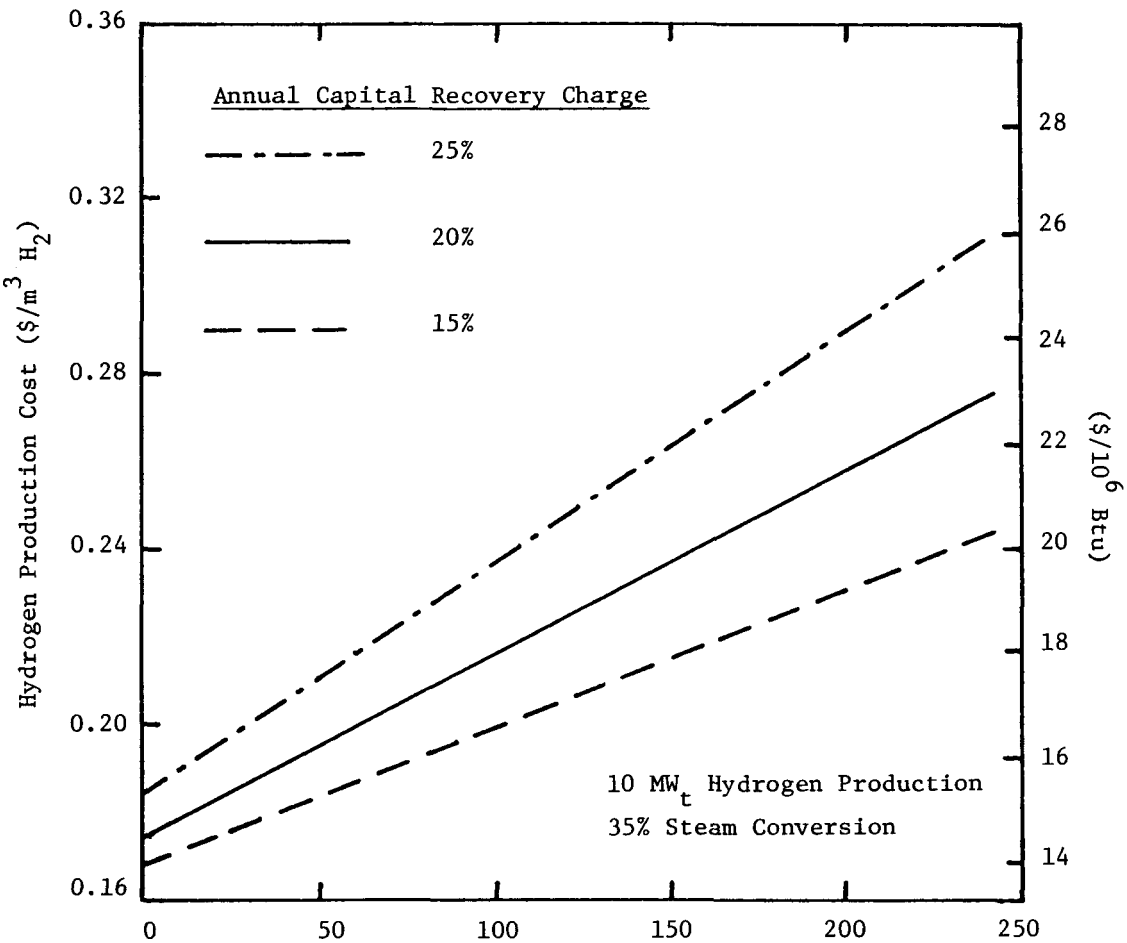

Hydrogen Production Cost as a Function of Electrolyzer Cost for Several Annual Capital Recovery Charges

MASSACHUSETTS INSTITUTE OF TECHNOLOGY SCHOOL OF CHEMICAL ENGINEERING PRACTICE			
DATE 8-30-83	DRAWN BY AB	FILE NO MIT-BNL-83-3	FIG 6-1

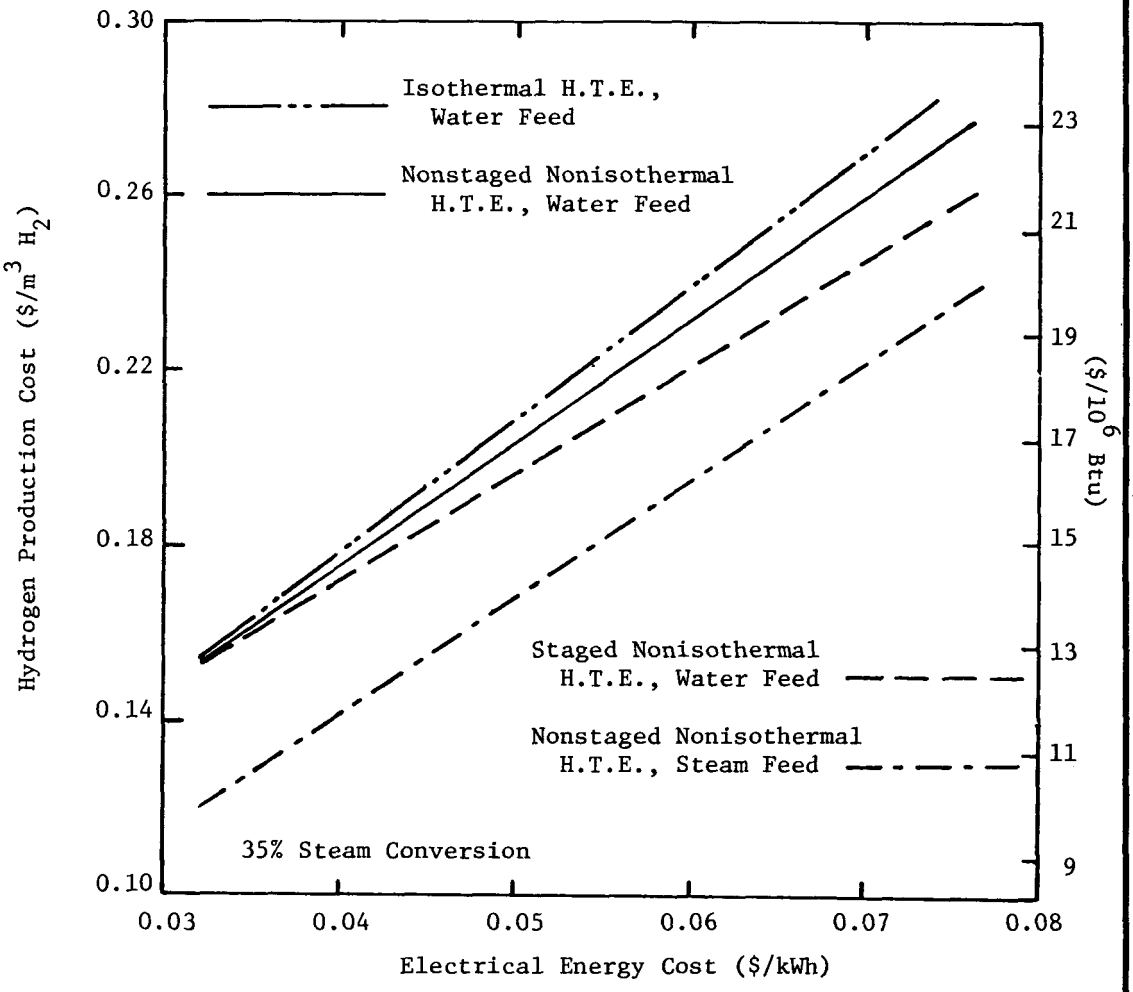

Hydrogen Production Cost as a Function of Electrical Energy Cost

MASSACHUSETTS INSTITUTE OF TECHNOLOGY SCHOOL OF CHEMICAL ENGINEERING PRACTICE			
DATE 8-30-83	DRAWN BY AB	FILE NO MIT-BNL-83-3	FIG. 6-2

A comparison of the hydrogen production costs obtained for each of the processes considered is shown in Table (6-1) for a 35% steam conversion. A 20% annual capital recovery charge, $50/kW_t$ H_2 electrolyzer cost, $0.05/kWh electrical power cost, and $2/10^6$ Btu thermal energy cost have been assumed. Among the water-fed processes, the one with staged nonisothermal electrolyzer operation provides the least expensive hydrogen product. This is due to the reduction in electrical power consumption obtained through staging (see Section 5.4). Lower electrical energy input results in lower hydrogen production cost because electricity at $0.05/kWh is over seven times more expensive than the thermal energy at $2/10^6$ Btu which replaces that electricity. A water-fed process with isothermal electrolyzer operation, on the other hand, produces the most expensive hydrogen product. Electrical resistance heating of the product streams in the electrolyzer results in higher electrical power consumption than a nonisothermal process, and thus in a higher hydrogen production cost.

Table (6-1)
Comparison of HTE Hydrogen Production Costs for a 35% Steam Conversion

Feed	Electrolyzer Operation	Production Cost ($/m^3 H_2)	Production Cost ($/$10^6$ Btu)
Water	Isothermal	0.21 - 0.22	17 - 18
Water	Nonstaged Nonisothermal	0.20 - 0.21	16 - 17
Water	Staged Nonisothermal	0.19 - 0.20	15 - 16
Steam	Isothermal	0.20 - 0.21 (0.22 - 0.23*)	16 - 17 (18 - 19*)
Steam	Nonstaged Nonisothermal	0.17 - 0.18 (0.19 - 0.20*)	14 - 15 (15 - 16*)

*Including Steam Cost of 0.69¢/kg ($3.10/1000 lbm).

Basis: Electrical Energy Cost = $0.05/kWh
Thermal Energy Cost = $2/10^6$ Btu
20% Annual Capital Recovery Charge
Hydrogen Product 10 MW_t, 25°C (77°F), 3 atm
Hydrogen Volume Measured at 0°C (32°F), 1 atm

6.2 Comparison of High-Temperature Steam Electrolysis with Other Hydrogen Production Processes

Typical hydrogen production costs for several hydrogen-producing processes are presented in Table (6-2). Hydrogen production costs obtained from two of the references were recalculated so that cost comparisons could be made on a common raw material cost basis [Corneil and Heinzelmann (1980) and Gregory et al. (1980)]. As can be seen from this table, steam reforming and partial oxidation of hydrocarbons are currently more economical than the HTE process. On the other hand, low-temperature water electrolysis processes are less economical than high-temperature steam electrolysis because of their higher electrical power consumption. Even the most efficient process under development, General Electric's solid-polymer electrolysis process, has a higher hydrogen production cost.

Table (6-2)
Comparison of Hydrogen Production Costs for HTE and Competing Processes

Process	Production Cost ($/m^3 H_2)	Production Cost ($/$10^6$ Btu)	Reference
Catalytic Steam Reforming of Natural Gas	0.07 - 0.10	6 - 8	Corneil and Heinzelmann (1980)
	0.08 - 0.11	7 - 9	Gregory et al. (1980)
	0.10 - 0.12	8 - 10	Beller (1983)
Partial Oxidation of Residual Fuel Oil	0.11 - 0.14	9 - 12	Gregory et al. (1980)
	0.12 - 0.16	10 - 13	Corneil and Heinzelmann (1980)
Koppers-Totzek Coal Gasification	0.14 - 0.17	12 - 14	Corneil and Heinzelmann (1980)
	0.17 - 0.20	14 - 16	Gregory et al. (1980)
High-Temperature Steam Electrolysis	0.17 - 0.22	14 - 18	This study
Advanced Solid-Polymer Electrolysis	0.22 - 0.24	18 - 20	Gupta and Russell (1981)
Conventional Electrolysis	0.34 - 0.41	28 - 34	Gregory et al. (1980)

Basis: Cost of Electricity = $0.05/kWh
Cost of Coal = $2/$10^6$ Btu
Cost of Natural Gas = $3.50/$10^6$ Btu
Cost of Residual Fuel Oil = $20/bbl
20% Annual Capital Recovery Charge
Hydrogen Volume Measured at 0°C (32°F), 1 atm

The production costs shown in Table (6-2) for the Koppers-Totzek coal gasification process are similar to our estimates for the HTE process. This is somewhat misleading because these coal gasification production costs were based on a 399-MW_t H_2 (1360 x 10^6 Btu/hr) plant capacity. The coal gasification, steam reforming, and partial oxidation processes all have significant reductions in production cost with increased plant size due to economies of scale [Gregory et al. (1980)]. At a 399-MW_t H_2 plant capacity, about three-fourths of the Koppers-Totzek hydrogen production cost of \$0.16 to \$0.18/m^3 H_2 produced (\$13 to \$15/10^6 Btu) is accounted for by the 20% annual capital recovery charge. Decreasing the plant capacity to 10 MW_t H_2 (34.1 x 10^6 Btu/hr) would cause the Koppers-Totzek hydrogen production cost to jump to about \$0.40 to \$0.46/m^3 H_2 (\$33 to \$38/10^6 Btu). Hydrogen production costs for the low- and high-temperature electrolysis processes are not strongly affected by plant size because electrolyzer cost is almost directly proportional to plant capacity.

Two of the three catalytic steam reforming hydrogen production cost estimates given in Table (6-2) were also based on a 399-MW_t H_2 plant capacity [Corneil and Heinzelmann (1980) and Gregory et al. (1980)]. In these two cases, only about one-third of the hydrogen production cost of \$0.08 to \$0.11/m^3 H_2 produced (\$7 to \$9/10^6 Btu) was accounted for by the capital recovery charge. As a result, decreasing the plant capacity to 10 MW_t H_2 only increases the steam reforming hydrogen production cost to about \$0.14 to \$0.18/m^3 H_2 (\$12 to \$15/10^6 Btu).

More significantly, about two-thirds of the catalytic steam reforming hydrogen production cost is accounted for by the cost of the natural gas feedstock. An increase in the cost of natural gas from \$3.50/10^6 Btu to \$8/10^6 Btu would increase the steam reforming hydrogen production cost from the value given in Table (6-2) (\$0.08 to \$0.11/m^3 H_2 produced) to about \$0.16 to \$0.20/m^3 H_2 (\$13 to \$17/10^6 Btu). This production cost is comparable to our HTE hydrogen production cost estimates of \$0.17 to \$0.22/m^3 H_2 produced (\$14 to \$18/10^6 Btu).

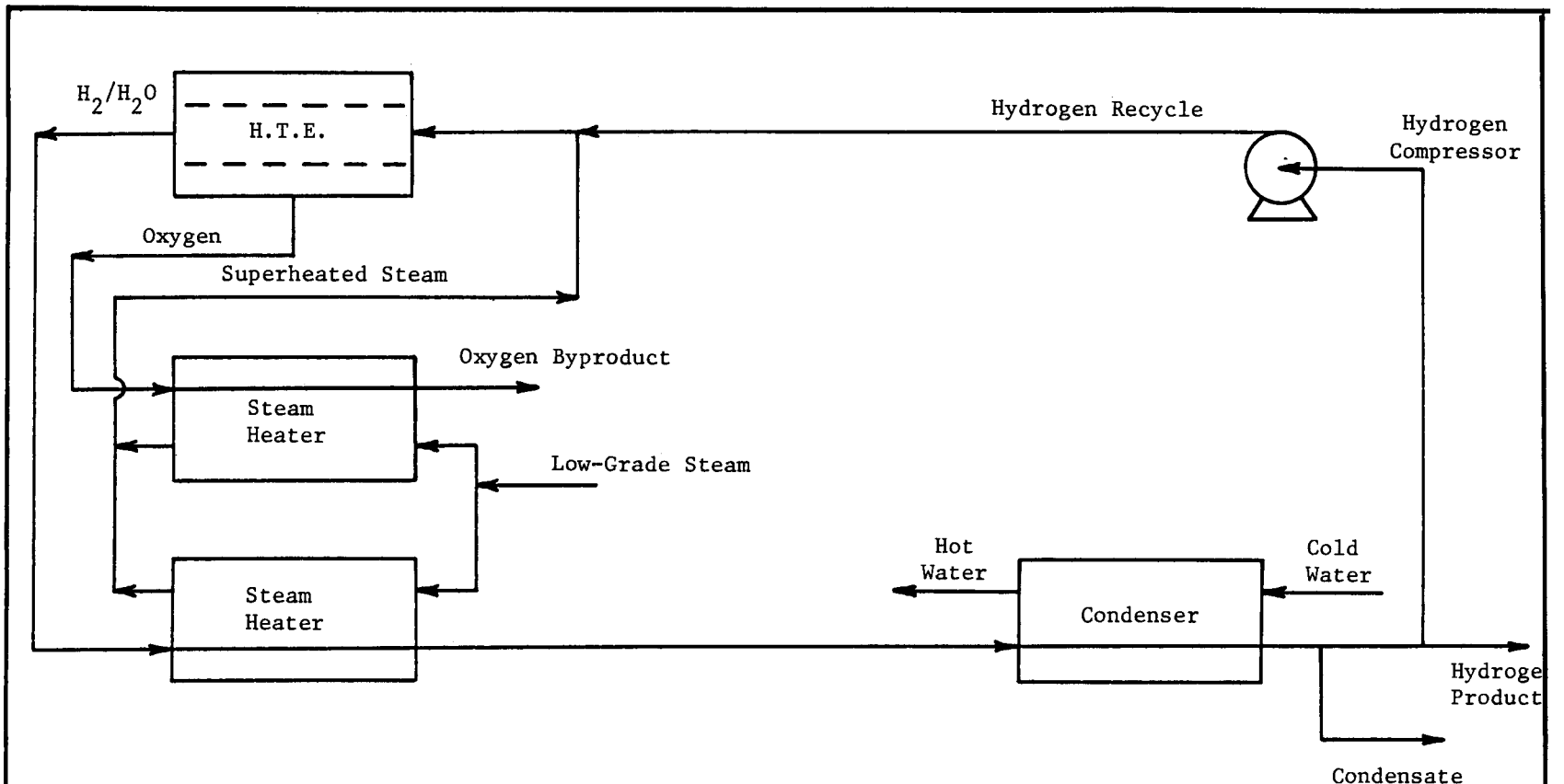

Process A: Steam Feed and Near-Isothermal H.T.E. Operation

MASSACHUSETTS INSTITUTE OF TECHNOLOGY SCHOOL OF CHEMICAL ENGINEERING PRACTICE	DATE 9-3-83	DRAWN BY MAL	FILE NO. MIT-BNL-83-3	FIG. 6-3a

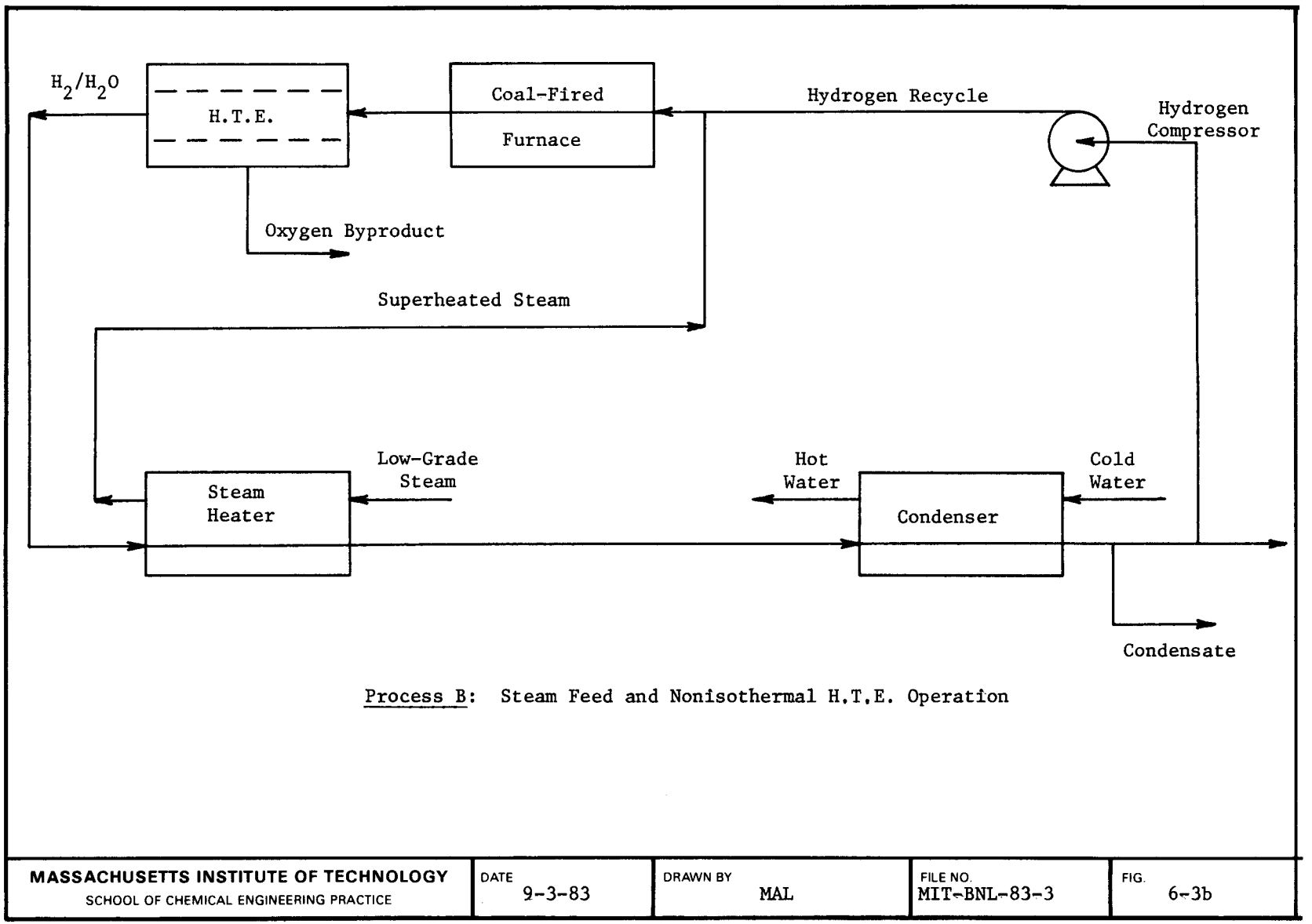

Process B: Steam Feed and Nonisothermal H.T.E. Operation

MASSACHUSETTS INSTITUTE OF TECHNOLOGY SCHOOL OF CHEMICAL ENGINEERING PRACTICE	DATE 9-3-83	DRAWN BY MAL	FILE NO. MIT-BNL-83-3	FIG. 6-3b

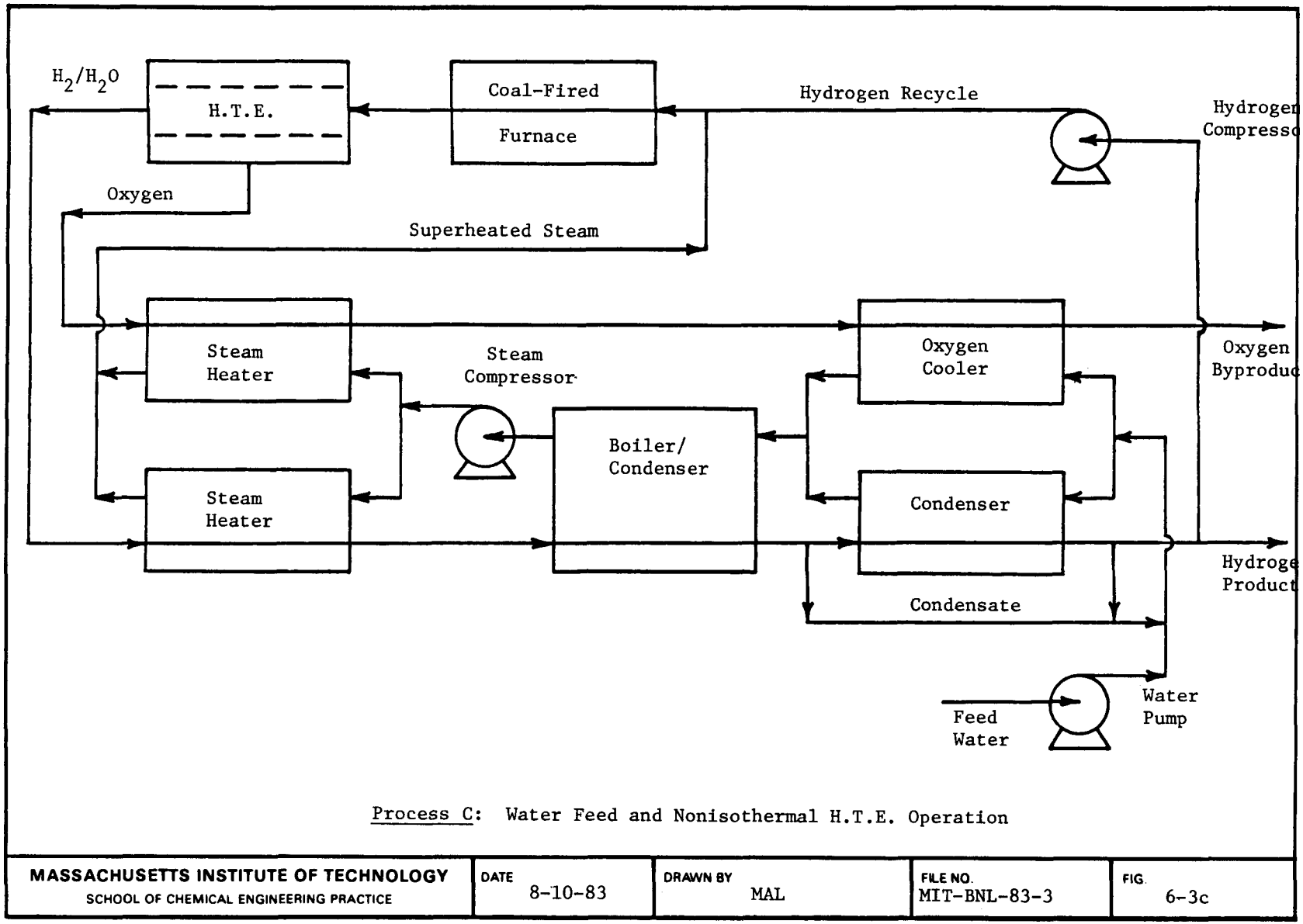

Process C: Water Feed and Nonisothermal H.T.E. Operation

MASSACHUSETTS INSTITUTE OF TECHNOLOGY SCHOOL OF CHEMICAL ENGINEERING PRACTICE	DATE 8-10-83	DRAWN BY MAL	FILE NO. MIT-BNL-83-3	FIG. 6-3c

7 CONCLUSIONS

(1) Several alternative high-temperature steam electrolysis (HTE) processes were selected. Hydrogen production costs for these processes were then estimated based on a technical analysis of the process flowsheets. Finally, the HTE hydrogen production cost estimates were compared with those for other hydrogen manufacturing processes.

(2) High-temperature electrolysis coupled with thermal and electrical energy derived from coal is not yet competitive with processes which make hydrogen from hydrocarbons. If natural gas costs were to double, however, catalytic steam reforming and HTE would have comparable hydrogen production costs.

(3) Electrical power cost is the major component of HTE hydrogen production cost. For electrolyzer steam conversions greater than about 50%, electrical power cost makes up about 80% of the hydrogen production cost.

(4) Replacement of electrical power input with thermal energy reduces HTE hydrogen production cost. Production cost reductions of 10% to 15% can be obtained in this way.

(5) The capital cost for a HTE process is only an important component of hydrogen production cost for low electrolyzer steam conversions. This gives HTE an advantage over coal gasification, where capital cost is the major component of production cost.

(6) High electrolyzer steam conversions give the best thermodynamic efficiency in converting coal-fired heat into hydrogen. A thermodynamic efficiency of 30.6% for a 15% steam conversion can be increased to 38.2% at a 90% conversion.

(7) The degree of heat recovery obtained has a strong effect on the thermodynamic efficiency of a HTE process. For a 30% electrolyzer steam conversion, a 31.1% thermodynamic efficiency can be increased to 38.5% with additional heat recovery equipment. Adding that equipment would increase capital cost, however.

8 RECOMMENDATIONS

We have the following recommendations:

(1) Continue development of high-temperature steam electrolysis (HTE) cells. HTE hydrogen production costs are lower then those for low-temperature electrolysis processes. They are also at least comparable to, or maybe even much lower than, those for coal gasification processes.

(2) Investigate the possibility of solid-oxide electrolytes with good oxygen-ion conductivity at about 600° to 700°C (1112° to 1292°F). This would eliminate the materials problems posed by operation near 1000°C (1832°F).

(3) Develop HTE cells with long operating lifetimes at high current densities. This would both ensure good electrolyzer reliability and reduce electrolyzer size, thereby decreasing the total capital investment required for a HTE plant.

(4) If HTE cells must be operated at very high temperatures, the feasibility of moderate-cost large-area superalloy heat exchangers operating at temperatures near 1000°C and pressures up to about 12 atm must be verified.

(5) Investigate the possibility of using a partially-combusted flue gas containing significant quantities of carbon monoxide to depolarize the anode of HTE cells, thus making a substantial reduction in the electrical power consumption of a HTE process coupled with a coal-fired heat source. Reducing use of electricity would in turn reduce hydrogen production cost.

9 ACKNOWLEDGMENTS

We thank our consultants George Skaperdas, Al Mezzina, and Frank Salzano for the constructive criticism and suggestions provided during our study. We also appreciate the technical input supplied by M. Beller, M. P. Manning, and H. P. Meissner.

One of us (MAL) acknowledges the support of the NSF Graduate Fellowship Program during this study.

10 APPENDIX

10.1 ASPEN-PLUS Flowsheet Models

The ASPEN-PLUS process simulator program [Aspen Technology, Inc. (1983)] was used to calculate material and energy balances for the alternative high-temperature steam electrolysis (HTE) process flowsheets. These balances were closed to within 0.01%, resulting in an error of less than about 0.05% in subsequent thermodynamic efficiency calculations.

The ASPEN-PLUS simulator divides a flowsheet into individual unit operation simulation blocks connected by material and energy streams. The block shown in Fig. (10-1) was used to simulate cooling of the steam-hydrogen product mixture. The different block types we used are given in Table (10-1). Each block and stream was given a unique name to aid analysis of the ASPEN-PLUS program output.

Table (10-1)
ASPEN-PLUS Unit Operation Simulation Blocks Used in This Study

Block Type	Function
HEATER	Stream heater/boiler or cooler/condenser
MIXER	Mixing of streams
COMPR	Gas compressor
FSPLIT	Splitting of complete streams
RSTOIC	Chemical reactor
SEP2	Splitting of stream components
PUMP	Liquid Pump

Figure (10-2) shows the flowsheet model used to simulate the steam-fed electrolysis processes. The electrolyzer was simulated by using an RSTOIC block and a SEP2 block in series. Energy balances were closed around two HEATER blocks connected by a heat stream in order to model adiabatic heat exchangers. An extra HEATER block called H2OBLR was added to the flowsheet to simplify the computational sequence by reboiling the water condensed from the steam-hydrogen product mixture.

The model used to simulate the water-fed processes is shown in Fig. (10-3). Three HEATER blocks called H2OCL2, H2OCL3, and H2OCL4 were used to simulate cooling towers by reducing the condensate temperature to 15°C

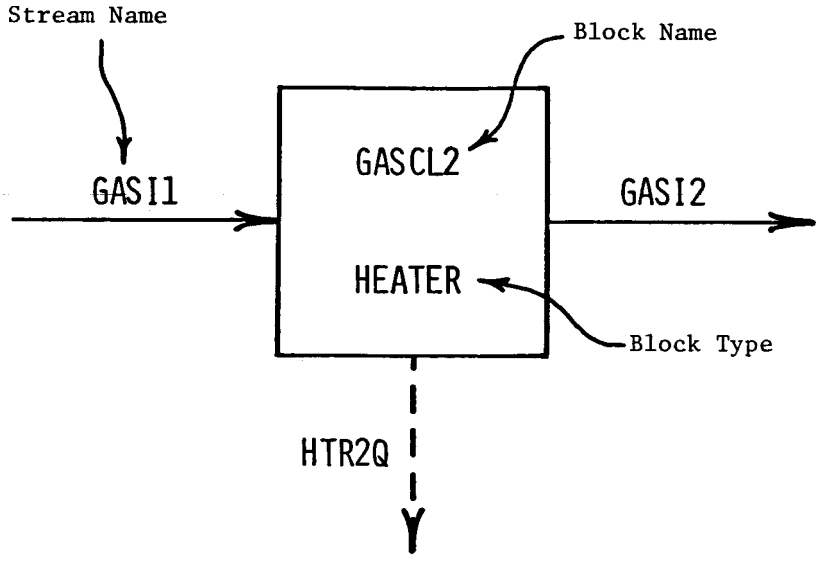

Material Stream

Energy Stream

Example Unit Operation Simulation Block

MASSACHUSETTS INSTITUTE OF TECHNOLOGY SCHOOL OF CHEMICAL ENGINEERING PRACTICE			
DATE 9-3-83	DRAWN BY MAL	FILE NO MIT-BNL-83-3	FIG 10-1

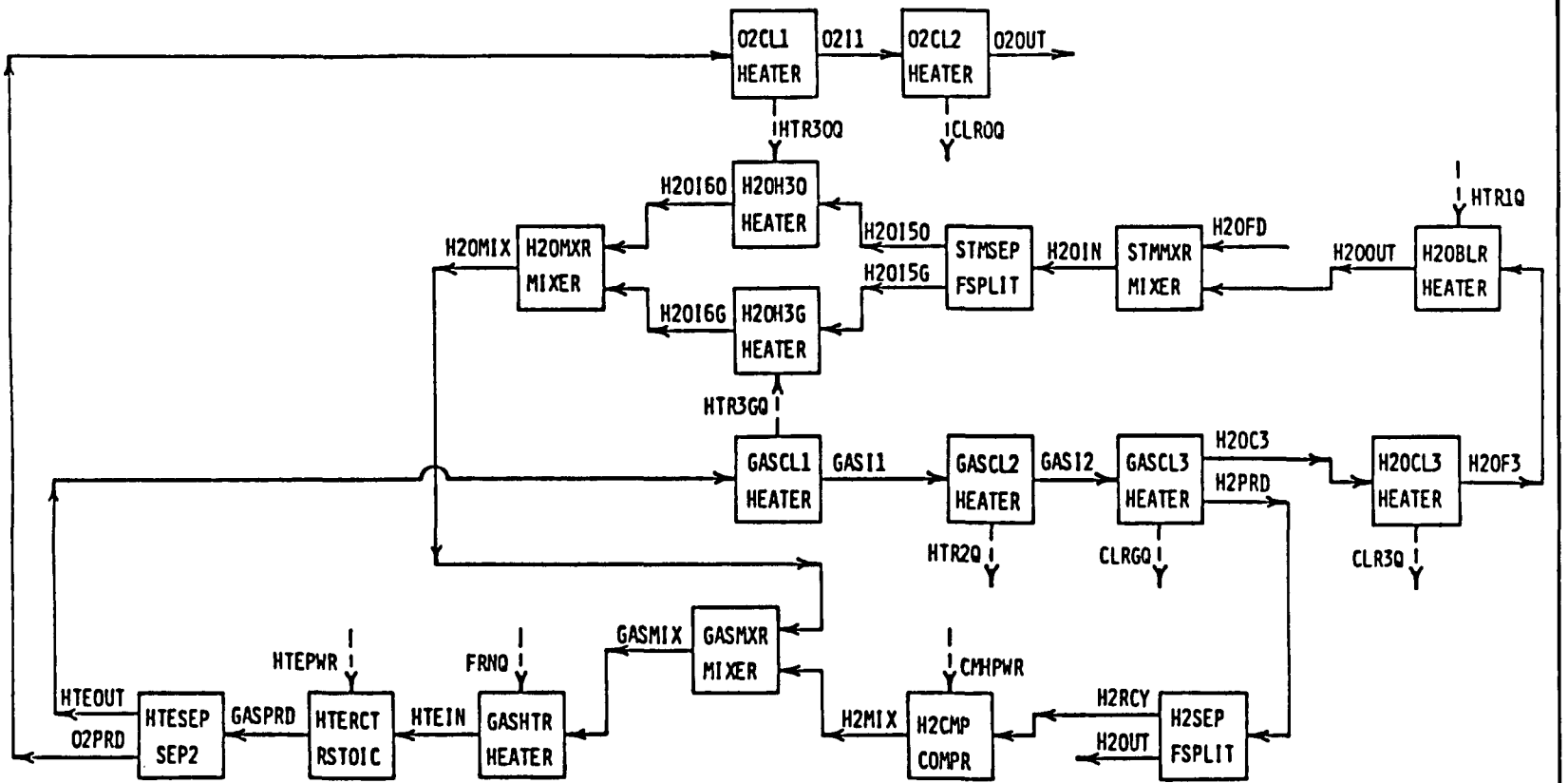

Computer Model for Steam-Fed H,T,E, Process

MASSACHUSETTS INSTITUTE OF TECHNOLOGY SCHOOL OF CHEMICAL ENGINEERING PRACTICE	DATE 9-4-83	DRAWN BY MAL	FILE NO. MIT-BNL-83-3	FIG. 10-2

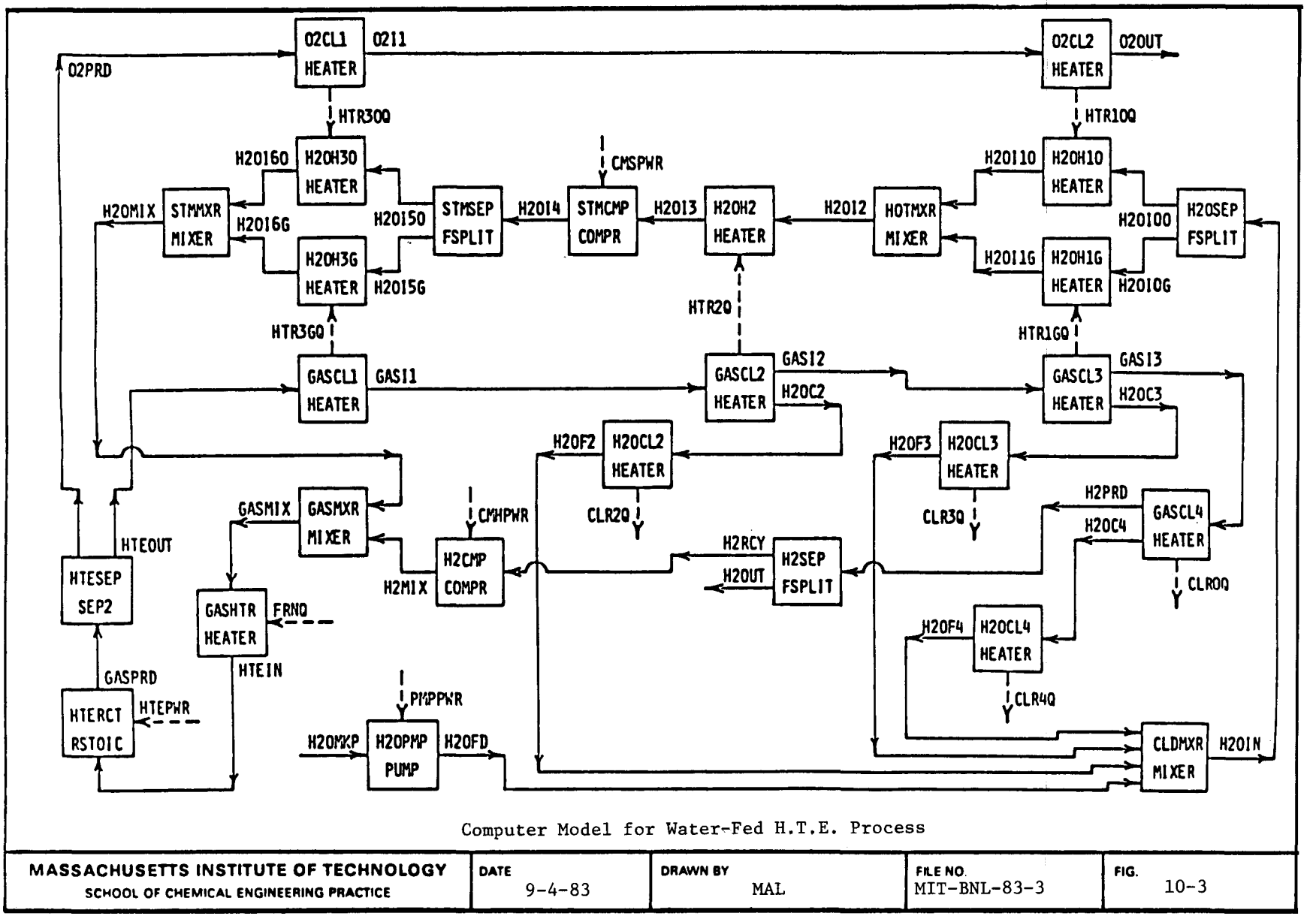

Computer Model for Water-Fed H.T.E. Process

MASSACHUSETTS INSTITUTE OF TECHNOLOGY SCHOOL OF CHEMICAL ENGINEERING PRACTICE	DATE 9-4-83	DRAWN BY MAL	FILE NO. MIT-BNL-83-3	FIG. 10-3

(59°F). Some blocks shown in Fig. (10-3) became unnecessary under certain operating conditions and were therefore not included when simulating operation under those conditions.

The ASPEN-PLUS simulator program is able to estimate nonideal gas and liquid mixture thermodynamic properties. We used the Redlich-Kwong equation of state to calculate nonideal gas mixture properties and an implementation of the 1967 ASME Steam Tables for pure steam and water properties.

10.2 Location of Original Calculations

Our original calculations are on file at the Brookhaven Station of the M.I.T. School of Chemical Engineering Practice, Building 475, Brookhaven National Laboratory, Upton, New York 11973. Input and output from our ASPEN-PLUS simulator runs are also available at the Brookhaven Station.

10.3 Nomenclature

A = heat transfer area, m^2.
E = reversible cell potential in electrolysis, V.
E' = actual cell potential in electrolysis, V.
F = Faraday constant, 9.65×10^7 J/V kequiv.
G = molar free energy, J/kmol.
ΔG = molar free energy change through electrolysis, J/kmol H_2O.
H = molar enthalpy, J/kmol.
ΔH = molar enthalpy change through electrolysis, J/kmol H_2O.
i = summation index.
m = steam flow rate, kmol/sec.
Δm = change in steam flow rate through electrolysis, kmol/sec.
n = electron transfer through electrolysis, 2 kequiv/kmol H_2O.
N = number of electrolysis cells in series.
Q = heat duty, W.
S = molar entropy, J/kmol K.
ΔS = molar entropy change through electrolysis, J/kmol H_2O K.
T = absolute temperature, K.
ΔT_m = log-mean temperature difference, K.
U = overall heat transfer coefficient, W/m^2 K.
W = electrolysis power, W.
x = mole fraction H_2.
Δx = change in H_2 mole fraction.

10.4 References

Aspen Technology, Inc., ASPEN PLUS Introductory Manual, Cambridge, MA (June 1983).

Beller, M., personal communication, Brookhaven National Laboratory, Upton, NY (August 1983).

Booth, L., Ed., "Fusion Energy Applied to Synthetic Fuel Production," Conf. 770593 (1979).

Corneil, H. G., and F. J. Heinzelmann, "Hydrogen in Oil Refinery Operations," in Hydrogen: Production and Marketing, ACS Symposium Series, 116, 67 (1980).

Doenitz, W., R. Schmidberger, E. Steinheil, and R. Streicher, "Hydrogen Production by High Temperature Electrolysis of Water Vapour," Int. J. Hydrogen Energy, 5, 55 (1980).

DVT-USA, "Unique Heavy-Duty Heat Exchanger is Now Available in the U.S.," Chem. Eng., 90 (15), 35 (July 25, 1983).

Fillo, J. A., Ed., "HYFIRE: Fusion/High Temperature Electrolysis Conceptual Design Study," BNL Report, in preparation, Upton, NY (1983).

Gregory, D. P., C. L. Tsaros, J. L. Arora, and P. Nevrekar, "The Economics of Hydrogen Production," in Hydrogen: Production and Marketing, ACS Symposium Series, 116, 3 (1980).

Gupta, D. K., and J. H. Russell, "Solid Polymer Electrolysis Economic and Design Study," DOE Contract No. DE-AC02-78ET26202, General Electric Company, Wilmington, MA (December 1981).

Holman, J. P., Heat Transfer, 5th Edition, McGraw-Hill Book Company, New York, NY (1981).

Isenberg, A. O., "Energy Conversion Via Solid Oxide Electrolyte Electrochemical Cells at High Temperatures," Solid State Ionics, 3/4, 431 (1981).

Kane, L., Ed., "Integral Heat Exchanger Design," Hydrocarbon Processing, 62 (7), 191 (July 1983).

Mandelik, B. G., and D. S. Newsome, "Hydrogen," in Kirk-Othmer Encyclopedia of Chemical Technology, 3rd Edition, 12, 938 (1980).

Marshall and Swift, "M S Equipment Cost Index," Chem. Eng., 90 (16), 7 (August 8, 1983).

Mezzina, A., "Visit Memo -- HTE Project Meetings at Westinghouse R D Center, Pittsburgh, PA -- March 28-29, 1983," BNL Memorandum, Upton, NY (March 31, 1983).

Mezzina, A., and M. Bonner, "Visit to Westinghouse R D -- August 3-4, 1983," BNL Memorandum, Upton, NY (August 5, 1983).

Perry, R. H., and C. H. Chilton, Chemical Engineers' Handbook, 5th Edition, McGraw-Hill Book Company, New York, NY (1973).

Peters, M.S., and K. D. Timmerhaus, Plant Design and Economics for Chemical Engineers, 3rd Edition, McGraw-Hill Book Company, New York, NY (1980).

Powell, J. R., "Fusion Reactors for Synthetic Fuels," Trans. Am. Nuc. Soc., 32, 17 (1979).

Westinghouse Electric Corporation, "Technical Progress Report No. 1: High Temperature Water Vapor Electrolysis Using Solid Electrolyte Cells," BNL Contract No. 585847-S, Pittsburgh, PA (May 6, 1983).

☆U.S. GOVERNMENT PRINTING OFFICE: 1984 717 032 10004